Supporting Information

Sebastián Martínez-Vivas, Macarena Poyatos and Eduardo Peris

Institute of Advanced Materials (INAM). Centro de Innovación en Química Avanzada (ORFEO-CINQA). Universitat Jaume I. Av. Vicente Sos Baynat s/n. Castellón. E-12071. Spain.

General considerations

Bis-imidazolium salt [**3**](I)$_2$[1] and N-(1-ethylpropyl)naphthalene-1,8-naphtalimide-4,5-dicarboxylic anhydride[2] were prepared as described in the literature. The solvents were dried using a solvent purification system (SPS M BRAUN) or purchased and degassed prior to use by purging them with dry nitrogen. All the other reagents were used as received from the commercial suppliers. Column chromatography was performed using silica gel (60-120 mesh). NMR spectra recorded on a Bruker 300 MHz using CD_2Cl_2, CD_3CN, CD_3OD or DMSO-d_6 as solvents, chemical shifts (δ) are expressed in ppm using the residual proton resonance of the solvent as an internal standard. All coupling constants (*J*) are expressed in hertz (Hz). Exact mass analysis was recorded by using a Q-TOF Premier mass spectrometer with an electrospray source (Waters, Manchester, UK) operating at a resolution of about 16000 FWHM. UV-Visible absorption spectra were recorded on a Varian Cary 300 BIO spectrophotometer under ambient conditions using 10^{-6} M concentrations of the compounds under study.

1. Synthesis and characterization of the compounds

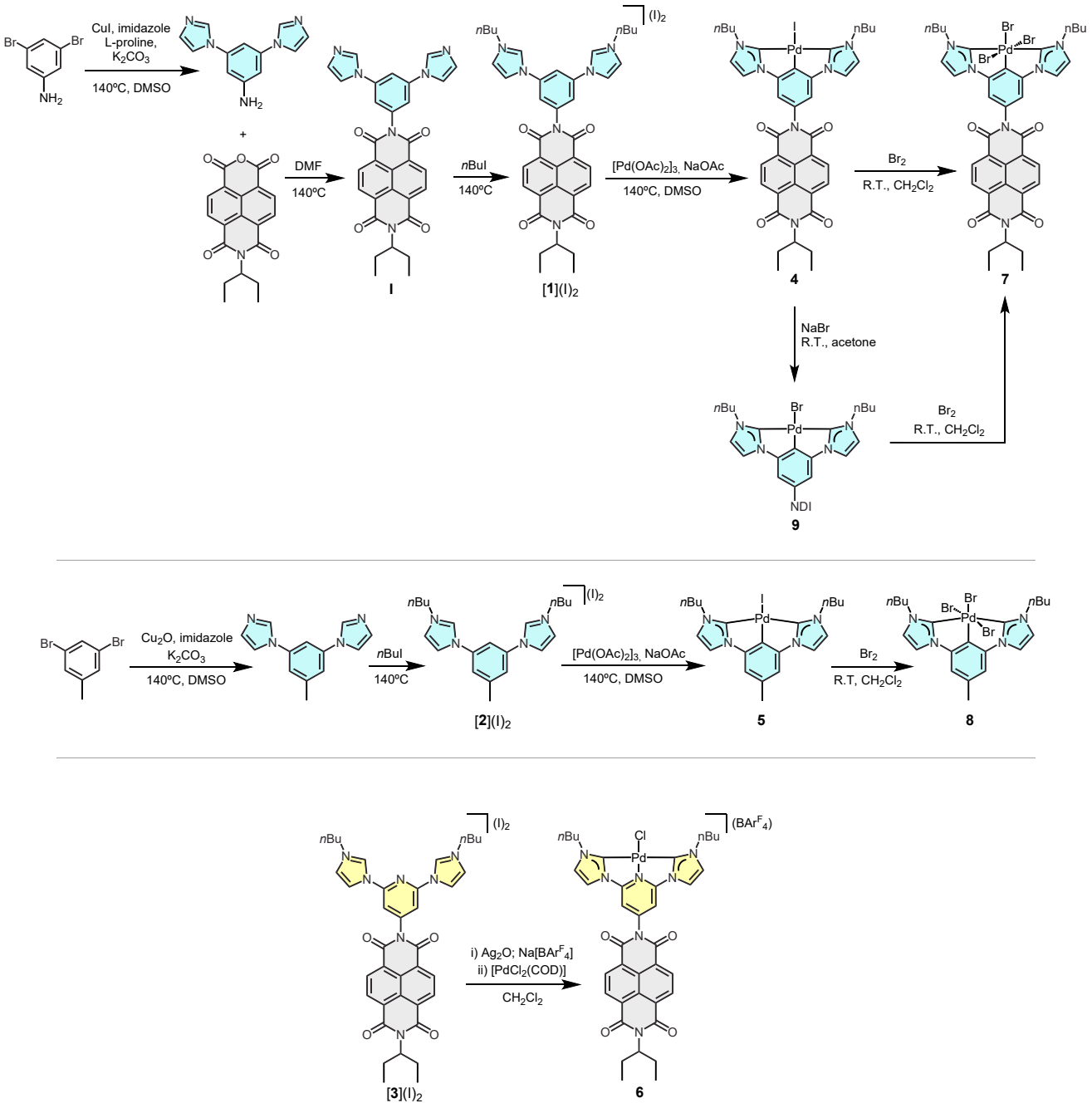

Scheme S1. Synthesis of the NHC-based pincer complexes described in this work

1.1. Synthesis of the precursors of the NHC ligands

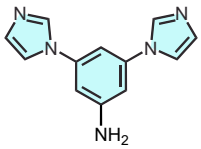

Synthesis of 3,5-bis(imidazol-1-yl)aniline. 3,5-Dibromoaniline (2.49 g, 9.92 mmol), imidazole (2.06 g, 30.26 mmol), L-proline (0.23 g, 2.00 mmol), K_2CO_3 (6.93 g, 50.1 mmol) and CuI (0.38 g, 2.00 mmol) were placed together in a round bottom flask. The solids were suspended in DMSO (15 mL) and stirred at 140 ºC overnight. Once at room temperature, the reaction mixture was diluted with water (250 mL). The resulting reaction mixture was extracted with EtOAc:*n*-BuOH (9:1) (4 x 250 mL). The combined organic phases were dried under vacuum and the solid obtained was washed with acetone. The desired product was isolated as an off-white solid in 79% yield (1.78 g). **^{1}H NMR** (300 MHz, CD_3OD): δ = 8.16 (s, 2H, NC*H*N), 7.59 (s, 2H, CH_{imid}), 7.15 (s, 2H, CH_{imid}), 7.00 (t, $^4J_{H\text{-}H}$ = 1.9 Hz, 1H, CH_{Ph}), 6.84 (d, $^4J_{H\text{-}H}$ = 1.9 Hz, 2H, CH_{Ph}). **^{13}C{^{1}H} NMR** (75 MHz, CD_3OD): δ =152.8 (C_{Ph}), 140.5 (C_{Ph}), 137.0 (N*C*HN), 130.1 (*C*H$_{imid}$), 119.7 (*C*H$_{imid}$), 106.4 (*C*H$_{Ph}$), 102.9 (*C*H$_{Ph}$). HRMS (20 V, m/z): 226.1092 $[M+H]^+$. (Calcd. for $[M+H]^+$: 226.1093).

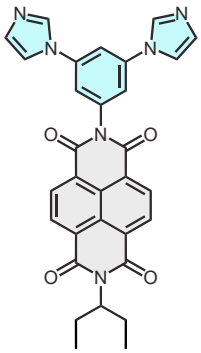

Synthesis and characterization of compound I. N-(1-Ethylpropyl)naphthalene-1,8-naphtalimide-4,5-dicarboxylic anhydride (300 mg, 0.889 mmol) was placed in a Schlenk tube fitted with a Teflon cap. The tube was evacuated and filled with nitrogen three times. The solid was dissolved in dry DMF (4 mL) and the mixture heated at 90 ºC under stirring conditions for 1h. 3,5-Bis(imidazol-1-yl)aniline (200 mg, 0.889 mmol) was added and the resulting mixture was further stirred at 140 ºC overnight. Once at room temperature, water was added resulting in the precipitation of a light-yellow solid. The solid was separated by filtration, washed with acetone and dried under vacuum. Compound **I** was isolated as a light-yellow solid in 61% yield (295 mg).**^{1}H NMR** (300 MHz, DMSO-d_6): δ = 8.75 (s, 4H, CH_{NDI}), 8.43 (s, 2H, NC*H*N), 8.19 (t, $^4J_{H\text{-}H}$ = 1.9 Hz, 1H, CH_{Ph}), 7.88 (s, 2H, CH_{imid}), 7.85 (d, $^4J_{H\text{-}H}$ = 2.0 Hz, 2H, CH_{Ph}), 7.18 (s, 2H, CH_{imid}), 4.99-4.85 (m, 1H, C*H*(CH$_2$CH$_3$)$_2$), 2.25-2.05 (m, 2H, CH(C*H*$_2$CH$_3$)$_2$), 1.98-1.83 (m, 2H, CH(C*H*$_2$CH$_3$)$_2$), 0.87 (t, $^3J_{H\text{-}H}$ = 7.4 Hz, 6H, CH(CH$_2$C*H*$_3$)$_2$). **^{13}C{^{1}H} NMR** (75 MHz, DMSO-d_6): δ= 162.7 (C=O$_{NDI}$), 135.8 (N*C*HN), 130.9 (*C*H$_{NDI}$), 130.3 (*C*H$_{imid}$), 126.6 (C_{NDI}),126.4, (C_{NDI}), 126.2 (C_{NDI}), 118.8 (*C*H$_{Ph}$), 118.0 (*C*H$_{imid}$), 57.4 (*C*H(CH$_2$CH$_3$)$_2$), 24.4 (CH(*C*H$_2$CH$_3$)$_2$), 11.2 (CH(CH$_2$*C*H$_3$)$_2$). HRMS (20 V, m/z): 545.1934 $[M+H]^+$. (Calcd. for $[M+H]^+$: 545.1937).

Synthesis and characterization of iodide salt [1](I)$_2$. Compound **I** (200 mg, 0.367 mmol)

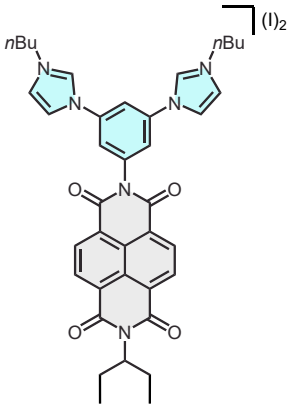

was reacted with an excess of n-butyl iodide (2 mL) in a Schlenk tube fitted with a Teflon cap. The mixture was heated at 140 ºC for 24 h. The addition of diethyl ether resulted in the precipitation of a solid that was collected by filtration and washed three times with diethyl ether. The compound was isolated as an orange solid in 60% yield (201 mg). **^{1}H NMR** (300 MHz, CD_3CN): δ = 10.08 (s, 2H, NC*H*N), 8.75 (s, 4H, CH_{NDI}), 8.64 (t, $^4J_{H\text{-}H}$ = 2.0 Hz, 1H, CH_{Ph}), 8.11 (t, $^3J_{H\text{-}H}$ = 1.9 Hz, 2H, CH_{imid}), 8.08 (d, $^4J_{H\text{-}H}$ = 2.0 Hz, 2H, CH_{Ph}), 7.66 (t, $^3J_{H\text{-}H}$ = 1.8 Hz, 2H, CH_{imid}), 5.05-4.95 (m, 1H, CH(CH_2CH_3)$_2$), 4.31 (t, $^3J_{H\text{-}H}$ = 7.3 Hz, 4H, C$H_2$$CH_2CH_2CH_3$), 2.29-2.11 (m, 2H, CH(C$H_2$$CH_3$)$_2$), 2.05-1.85 (m, 6H; 2H, CH(C$H_2$$CH_3$)$_2$ and 4H, CH_2C$H_2$$CH_2CH_3$), 0.98 (t, $^3J_{H\text{-}H}$ = 7.3 Hz, 6H, $CH_2CH_2CH_2$CH_3), 0.91 (t, $^3J_{H\text{-}H}$ = 7.5 Hz, 6H, CH(CH_2CH_3)$_2$). **^{13}C{^{1}H} NMR** (75 MHz, $CDCl_3$): δ 164.0 (C=O$_{NDI}$), 140.0 (*C*$_{Ph}$), 137.4 (*C*$_{Ph}$), 136.7 (N*C*HN), 132.0 (*C*H$_{NDI}$), 128.2 (*C*$_{NDI}$), 128.0 (*C*$_{NDI}$), 127.2 (*C*$_{NDI}$), 125.1 (*C*H$_{Ph}$),124.6 (*C*H$_{imid}$), 122.5 (*C*H$_{imid}$), 117.6 (*C*H$_{Ph}$), 59.0 (*C*H(CH_2CH_3)$_2$), 51.1 (*C*$H_2CH_2CH_2CH_3$), 32.3 (CH_2*C*$H_2CH_2CH_3$), 25.7 (CH(*C*H_2CH_3)$_2$), 20.0 (CH_2CH_2*C*H_2CH_3), 13.7 ($CH_2CH_2CH_2$*C*H_3), 11.6 (CH(CH_2*C*H_3)$_2$). HRMS (20 V, m/z): 329.1634 [M-2I]$^{2+}$. (Calcd. for [M-2I]$^{2+}$: 329.1634).

Synthesis of 3,5-bis(imidazol-1-yl)toluene. 3,5-Dibromotoluene (2.00 g, 8.00 mmol),

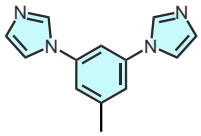

imidazole (1.36 g, 20.00 mmol), K_2CO_3 (4.42 g, 32.00 mmol) and Cu_2O (114.5 mg, 0.80 mmol)) were placed together in a round bottom flask. The solids were suspended in DMSO (15 mL) and stirred at 140 ºC overnight. After this time, the solvent was removed by distillation. The resulting solid was dissolved in CH_2Cl_2, filtered through a pad of Celite, and the solvent was removed under vacuum. The compound was isolated as a white solid in 78% yield (1.40 g). **^{1}H NMR** (300 MHz, CD_2Cl_2): δ = 7.88 (s, 2H, NC*H*N), 7.35 (s, 2H, CH_{imid}), 7.26 (m, 1H, CH_{Ph}), 7.25 (m, 2H, CH_{Ph}), 7.18 (s, 2H, CH_{imid}), 2.49 (s, 3H, CH_3). **^{13}C{^{1}H} NMR** (75 MHz, CD_2Cl_2): δ 142.9 (*C*$_{Ph}$), 139.1 (*C*$_{Ph}$), 136.1 (N*C*HN), 131.1 (*C*H$_{imid}$), 121.2 (*C*H$_{Ph}$), 118.7 (*C*H$_{imid}$), 112.1 (*C*H$_{Ph}$), 21.8 (*C*H_3). HRMS (20 V, m/z): 225.1146 [M+H]$^+$. (Calcd. for [M]$^+$: 225.2691).

Synthesis and characterization of iodide salt [2](I)$_2$. 3,5-Bis(imidazol-1-yl)toluene

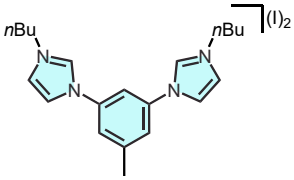

(200 mg, 0.891 mmol) was reacted with an excess of n-butyl iodide

(2 mL) in a Schlenk tube fitted with a Teflon cap. The mixture was heated at 140 ºC for 24 h. The addition of diethyl ether resulted in the precipitation of a solid that was collected by filtration and washed three times with diethyl ether. The desired product was isolated as an orange solid in 67% yield (356 mg). **^{1}H NMR** (300 MHz, CD_3CN): δ = 10.15 (s, 2H, NC*H*N), 8.28 (s, 1H, CH_{Ph}), 8.14 (s, 2H, CH_{imid}), 7.79 (d, $^{4}J_{H\text{-}H}$ = 0.8 Hz, 2H, CH_{Ph}), 7.65 (s, 2H, CH_{imid}), 4.32 (t, $^{3}J_{H\text{-}H}$ = 7.3 Hz, 4H, CH_2CH$_2$CH$_2$CH$_3$), 2.56 (s, 3H, CH_3), 1.99 (quint, $^{3}J_{H\text{-}H}$ = 7.4 Hz, 4H, CH$_2$CH_2CH$_2$CH$_3$), 1.44 (sext, $^{3}J_{H\text{-}H}$ = 7.6 Hz, 4H, CH$_2$CH$_2$CH_2CH$_3$), 0.98 (t, $^{3}J_{H\text{-}H}$ = 7.3 Hz, 6H, CH$_2$CH$_2$CH$_2$CH_3). **^{13}C{^{1}H} NMR** (75 MHz, CD_3CN): δ 142.7 (C_{Ph}), 134.9 (C_{Ph}), 134.7 (CH$_{imid}$), 122.7 (CH$_{Ph}$), 122.6 (CH$_{imid}$), 120.5 (CH$_{imid}$), 112.6 (CH$_{ph}$), 49.2 (CH$_2$CH$_2$CH$_2$CH$_3$), 30.6 (CH$_2$$CH_2CH_2CH_3$), 19.6 ($CH_3$), 18.3 (CH$_2CH_2$$CH_2CH_3$), 11.9 (CH$_2CH_2CH_2$$CH_3$). HRMS (20 V, m/z): 465.1524 $[M\text{-}I]^{+}$, 169.1235 $[M\text{-}2I]^{2+}$. (Calcd. for $[M\text{-}I]^{+}$: 465.3941, $[M\text{-}2I]^{2+}$: 169.2449).

1.2. Synthesis of the Pd(II) complexes

General route to complexes 4 and 5. The corresponding bis-imidazolium salt (1 equiv.), $Pd(OAc)_2$ (1.0 equiv.) and NaOAc (4.5 equiv.) were placed together in a round bottom flask. The solids were suspended in DMSO (8 mL) and stirred at 140 ºC overnight. After this time, the solvent was removed by vacuum distillation, and the resulting solid was dissolved in CH_2Cl_2. The solution was then filtered through Celite, and the solvent was removed under reduced pressure, yielding the desired complex.

Synthesis and characterization of complex 4. Complex **4** was prepared employing the general procedure by reacting [**1**](I)$_2$ (200 mg, 0.219 mmol), $Pd(OAc)_2$ (49 mg, 0.219 mmol) and NaOAc (82 mg, 1 mmol). Complex **4** was isolated as red solid in 39% yield (68 mg). **^{1}H NMR** (300 MHz, $CDCl_3$): δ = 8.79 (m, 4H, CH_{NDI}), 7.29 (d, $^3J_{H\text{-}H}$ = 1.5 Hz, 2H, CH_{imid}), 6.92 (d, $^3J_{H\text{-}H}$ = 1.5 Hz, 2H, CH_{imid}), 6.89 (s, 2H, CH_{Ph}), 5.10-5.00 (m, 1H, CH(CH_2CH$_3$)$_2$), 4.84 (t, $^3J_{H\text{-}H}$ = 5.6 Hz, 4H, CH_2CH$_2$CH$_2$CH$_3$), 2.29-2.18 (m, 2H, CH(CH_2CH$_3$)$_2$), 2.00-1.85 (m, 6H; 2H, CH(CH_2CH$_3$)$_2$ and 4H, CH$_2$CH_2CH$_2$CH$_3$), 1.49 (sext, $^3J_{H\text{-}H}$ = 5.8 Hz, 4H, CH$_2$CH$_2$CH_2CH$_3$), 0.97 (t, $^3J_{H\text{-}H}$ = 5.5 Hz, 6H, CH$_2$CH$_2$CH$_2$CH_3), 0.92 (t, $^3J_{H\text{-}H}$ = 5.6 Hz, 6H, CH(CH$_2$CH_3)$_2$). **^{13}C{^{1}H} NMR** (75 MHz, $CDCl_3$): δ = 176.1 (N*C*N), 163.3 (*C*=O$_{NDI}$), 147.7 (*C*$_{Ph}$), 146.2 (*C*$_{Ph}$), 131.8 (*C*H$_{NDI}$), 131.6 (*C*H$_{NDI}$), 127.2 (*C*$_{NDI}$), 127.1 (*C*$_{NDI}$), 126.5 (*C*$_{NDI}$), 120.8 (*C*H$_{imid}$), 114.2 (*C*H$_{imid}$), 108.8 (*C*H$_{Ph}$), 58.5 (*C*H(CH$_2$CH$_3$)$_2$), 51.9 (*C*H$_2$CH$_2$CH$_2$CH$_3$), 34.3 (CH$_2$*C*H$_2$CH$_2$CH$_3$), 25.1 (CH(*C*H$_2$CH$_3$)$_2$), 19.7 (CH$_2$CH$_2$*C*H$_2$CH$_3$), 14.1 (CH$_2$CH$_2$CH$_2$*C*H$_3$), 11.4 (CH(CH$_2$*C*H$_3$)$_2$). HRMS (20 V, m/z): 761.2077 [M-I]$^+$. (Calcd. for [M-I]$^+$: 761.2082).

Synthesis and characterization of complex 5. Complex **5** was prepared employing the general procedure by reacting [**2**](I)$_2$ (200 mg, 0.338 mmol), $Pd(OAc)_2$ (75 mg, 0.338 mmol) and NaOAc (125 mg, 1.5 mmol). Complex **5** was isolated as red solid in 45% yield (86 mg). **^{1}H NMR** (300 MHz, $CDCl_3$): δ = 7.30 (d, $^3J_{H\text{-}H}$ = 2.0 Hz, 2H, CH_{imid}), 6.90 (d, $^3J_{H\text{-}H}$ = 2.0 Hz, 2H, CH_{imid}), 6.72 (d, $^4J_{H\text{-}H}$ = 0.5 Hz, 2H, CH_{ph}), 4.80 (t, $^3J_{H\text{-}H}$ = 7.4 Hz, 4H, CH_2CH$_2$CH$_2$CH$_3$), 2.37 (s, 3H, CH_3), 1.86 (quint, $^3J_{H\text{-}H}$ = 7.6 Hz, 4H, CH$_2$CH_2CH$_2$CH$_3$), 1.48 (sext, $^3J_{H\text{-}H}$ = 7.8 Hz, 4H,

$CH_2CH_2CH_2CH_3$), 0.95 (t, $^3J_{H\text{-}H}$ = 7.3 Hz, 6H, $CH_2CH_2CH_2CH_3$). HRMS (20 V, m/z): 441.1284 $[M\text{-}I]^+$. (Calcd. for $[M\text{-}I]^+$: 441.1380).

Synthesis and characterization of complex 6. Iodide salt [**3**]$(I)_2$ (200 mg, 0.219 mmol),

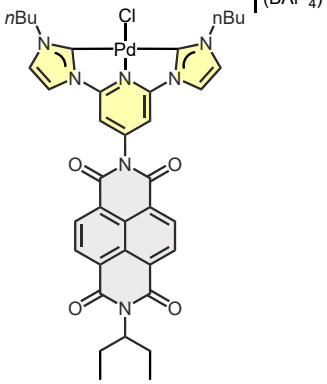

$Na(BAr^F{}_4)$ (213.5 mg, 0.241 mmol) and Ag_2O (50.7 mg, 0.219 mmol) were placed together in a Schlenk tube fitted with a Teflon cap. The tube was evacuated and filled with nitrogen three times. The solids were suspended in CH_2Cl_2 (4 mL) and stirred at room temperature in the absence of light overnight. After this time, the suspension was filtered through Celite into a flask charged with $[PdCl_2(COD)]$ (62.3 mg, 0.219 mmol). The suspension was stirred for 2 h and then passed through a column chromatography using dichloromethane as eluent. Complex **6** was isolated as an off-white yellow in 30% yield (108 mg). **^{1}H NMR** (300 MHz, CD_2Cl_2): δ = 8.82 (s, 4H, CH_{NDI}), 7.75-7.65 (m, 8H, Ar^F), 7.60 (d, $^3J_{H\text{-}H}$ = 2.1 Hz, CH_{imid}), 7.58 (s, 2H, CH_{pyr}), 7.54 (br, 4H, Ar^F), 7.20 (d, $^3J_{H\text{-}H}$ = 2.1 Hz, CH_{imid}), 5.10-4.98 (m, 1H, $CH(CH_2CH_3)_2$), 4.64 (t, $^3J_{H\text{-}H}$ =7.4 Hz, 6H, $CH_2CH_2CH_2CH_3$), 2.32-2.16 (m, 4H, $CH(CH_2CH_3)_2$), 2.05-1.90 (m, 6H; 2H, $CH(CH_2CH_3)_2$ and 4H, $CH_2CH_2CH_2CH_3$), 1.54-1.44 (m ,4H, $CH_2CH_2CH_2CH_3$), 1.01 (t, $^3J_{H\text{-}H}$ = 7.3 Hz, 6H, $CH_2CH_2CH_2CH_3$), 0.93 (t, $^3J_{H\text{-}H}$ = 7.5 Hz, 6H, $CH(CH_2CH_3)_2$). **^{13}C{^{1}H} NMR** (75 MHz, CD_2Cl_2): δ = 162.7 (C=O_{NDI}), 162.3 (q, $^1J_{CB}$ = 49.5 Hz, Ar^F), 152.2 ($C_{pyr\text{-}imid}$), 152.2 ($C_{pyr\text{-}NDI}$), 135.4 (Ar^F), 132.8 (CH_{NDI}), 129.7 (q, $^2J_{CF}$ = 2.9 Hz, Ar^F), 129.2 (q, $^1J_{CF}$ = 2.8 Hz, Ar^F), 124.7 (CH_{imid}), 118.0 (sept, $^3J_{FC}$ = 3.6 Hz, Ar^F), 117.4 (CH_{imid}), 110.1 (CH_{pyr}), 59.1 ($CH(CH_2CH_3)_2$), 51.1 ($CH_2CH_2CH_2CH_3$), 33.6 ($CH_2CH_2CH_2CH_3$), 25.5 ($CH(CH_2CH_3)_2$), 20.1 ($CH_2CH_2CH_2CH_3$), 13.9 ($CH_2CH_2CH_2CH_3$), 11.6 ($CH(CH_2CH_3)_2$).

Synthesis and characterization of complex 9. Complex **9** was prepared by reacting **4**

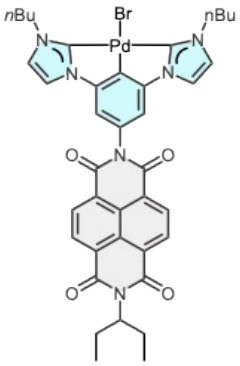

(100 mg, 0.110 mmol) with NaBr (23 mg, 0.220 mmol) in acetone. The reaction mixture was stirred at ambient temperature for 12 hours. After this time, all volatiles were removed *in vacuo*. The resulting solid was dissolved in CH_2Cl_2. The mixture was then filtered through Celite, and the solvent was removed under reduced pressure, yielding the product as a red solid in nearly quantitative yield. **^{1}H NMR** (300 MHz, $CDCl_3$): δ = 8.79 (m, 4H, CH_{NDI}), 7.28 (d, $^3J_{H\text{-}H}$ = 1.5 Hz, 2H, CH_{imid}), 6.92 (s,

2H, CH_{Ph}), 6.91 (d, $^3J_{H-H}$ = 1.5 Hz, 2H, CH_{imid}), 5.10-5.00 (m, 1H, CH(CH_2CH_3)$_2$), 4.77 (t, $^3J_{H-H}$ = 5.6 Hz, 4H, C$H_2$$CH_2CH_2CH_3$), 2.29-2.18 (m, 2H, CH(C$H_2$$CH_3$)$_2$), 2.00-1.85 (m, 6H; 2H, CH(C$H_2$$CH_3$)$_2$ and 4H, CH_2C$H_2$$CH_2CH_3$), 1.47 (m , 4H, CH_2CH_2C$H_2$$CH_3$), 0.96 (t, $^3J_{H-H}$ = 5.5 Hz, 6H, $CH_2CH_2CH_2$CH_3), 0.93 (t, $^3J_{H-H}$ = 5.6 Hz, 6H, CH(CH_2CH_3)$_2$). **^{13}C{^{1}H} NMR** (75 MHz, $CDCl_3$): δ = 176.0 (NCN), 163.4 (C=O_{NDI}), 147.8 (C_{Ph}), 146.1 (C_{Ph}), 131.8 (CH_{NDI}), 131.6 (CH_{NDI}), 127.2 (C_{NDI}), 127.1 (C_{NDI}), 126.5 (C_{NDI}), 120.8 (CH_{imid}), 114.2 (CH_{imid}), 108.9 (CH_{Ph}), 58.5 (CH(CH_2CH_3)$_2$), 52.0 ($CH_2CH_2CH_2CH_3$), 34.3 ($CH_2CH_2CH_2CH_3$), 25.1 (CH(CH_2CH_3)$_2$), 19.7 ($CH_2CH_2CH_2CH_3$), 14.1 ($CH_2CH_2CH_2CH_3$), 11.5 (CH(CH_2CH_3)$_2$). HRMS (20 V, m/z): 761.2097 $[M-Br]^+$. (Calcd. for $[M-Br]^+$: 761.2082).

1.3. Synthesis of the Pd(IV) complexes. General procedure

Br_2 (3.2 equiv.) was added to a solution of the corresponding Pd(II) complex (1 equiv.) in dichloromethane (2 mL). The reaction mixture was stirred at room temperature for 5 minutes. All the volatiles were removed *in vacuo*. The crude product was washed with diethyl ether affording an orange solid in all cases. Under these reaction conditions, the Pd(II) to Pd(IV) oxidation was successful for complexes **4** and **5**, which led to the formation of complexes **7** and **8**, respectively. However, the reaction of CNC-Pd(II) complex **6** with Br_2 did not yield the desired Pd(IV) complex and it was recovered unreacted.

Synthesis and characterization of complex 7. Complex **7** was prepared employing the general procedure by reacting complex **4** (30 mg, 0.0376 mmol) with Br_2 (6 µL, 0.12 mmol) in dichloromethane. The reaction mixture was evaporated to dryness *in vacuo* and the obtained solid was washed with diethyl ether. Complex **7** was isolated in 85% yield (30 mg). **^{1}H NMR** (300 MHz, $CDCl_3$): δ = 8.81 (m, 4H, CH_{NDI}), 7.64 (d, $^3J_{H-H}$ = 1.5 Hz, 2H, CH_{imid}), 7.28 (s, 2H, CH_{Ph}), 7.27 (d, $^3J_{H-H}$ = 1.5 Hz, 2H, CH_{imid}), 5.10-5.00 (m, 1H, CH(CH_2CH_3)$_2$), 4.80 (t, $^3J_{H-H}$ = 5.6 Hz, 4H, C$H_2$$CH_2CH_2CH_3$), 2.29-2.18 (m, 2H, CH(C$H_2$$CH_3$)$_2$), 2.10-1.85 (m, 6H; 2H, CH(C$H_2$$CH_3$)$_2$ and 4H, CH_2C$H_2$$CH_2CH_3$), 1.53 (sext, $^3J_{H-H}$ = 5.7 Hz, 4H, CH_2CH_2C$H_2$$CH_3$), 1.03 (t, $^3J_{H-H}$ = 5.5 Hz, 6H, $CH_2CH_2CH_2$CH_3), 0.93 (t, $^3J_{H-H}$ = 5.6 Hz, 6H, CH(CH_2CH_3)$_2$). **^{13}C{^{1}H} NMR** (75 MHz, $CDCl_3$): δ = 163.1 (*C*=O_{NDI}), 162.2 (N*C*N), 141.8 (*C*$_{Ph}$), 135.0 (*C*$_{Ph-Pd}$), 131.8 (*C*H$_{NDI}$), 131.3 (*C*H$_{NDI}$), 127.2 (*C*$_{NDI}$), 127.1 (*C*$_{NDI}$), 126.1(*C*$_{NDI}$), 123.3 (*C*H$_{imid}$), 117.3 (*C*H$_{imid}$), 116.5 (*C*$_{Ph}$) 112.8 (*C*H$_{Ph}$), 58.5 (*C*H(CH_2CH_3)$_2$), 51.5 (*C*$H_2CH_2CH_2CH_3$), 33.8 (CH_2*C*$H_2CH_2CH_3$), 25.1 (CH(*C*H_2CH_3)$_2$), 19.9 (CH_2CH_2*C*H_2CH_3), 14.0 ($CH_2CH_2CH_2$*C*H_3), 11.5 (CH(CH_2*C*H_3)$_2$). HRMS (20 V, m/z): 921.0453 [M-Br]$^+$. (Calcd. for [M-Br]$^+$: 921.0430).

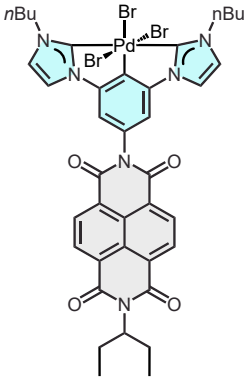

Synthesis and characterization of complex 8. Complex **8** was prepared employing the general procedure by reacting complex **5** (22 mg, 0.0376 mmol) with Br_2 (6 µL, 0.12 mmol) in dichloromethane. The reaction mixture was evaporated to dryness *in vacuo* and the obtained solid was washed with diethyl ether. Complex **8** was isolated in 80% yield (17 mg). **^{1}H NMR**

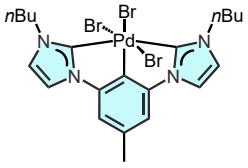

(300 MHz, $CDCl_3$): δ =7.61 (d, $^3J_{H\text{-}H}$ = 1.8 Hz, 2H, CH_{imid}), 7.14 (d, $^3J_{H\text{-}H}$ = 1.8 Hz, 2H, CH_{imid}), 7.06 (s, 2H, CH_{Ph}), 4.78 (t, $^3J_{H\text{-}H}$ = 7.6 Hz, 4H, CH_2CH$_2$CH$_2$CH$_3$), 2.59 (s, 3H, CH_3), 2.03 (quint, $^3J_{H\text{-}H}$ = 7.6 Hz, 4H, CH$_2$CH_2CH$_2$CH$_3$), 1.53 (sext, $^3J_{H\text{-}H}$ = 7.6 Hz, 4H, CH$_2$CH$_2$CH_2CH$_3$), 1.02 (t, $^3J_{H\text{-}H}$ = 7.3 Hz, 6H, CH$_2$CH$_2$CH$_2$CH_3). The instability of the complex prevented its characterization by $^{13}C\{^1H\}$ NMR. HRMS (20 V, m/z): 600.9625 [M-Br]$^+$. (Calcd. for [M-Br]$^+$: 601.7010).

2. Spectroscopic data

2.1. ^{1}H and $^{13}C\{^{1}H\}$ NMR spectra of 3,5-bis(imidazol-1-yl)aniline

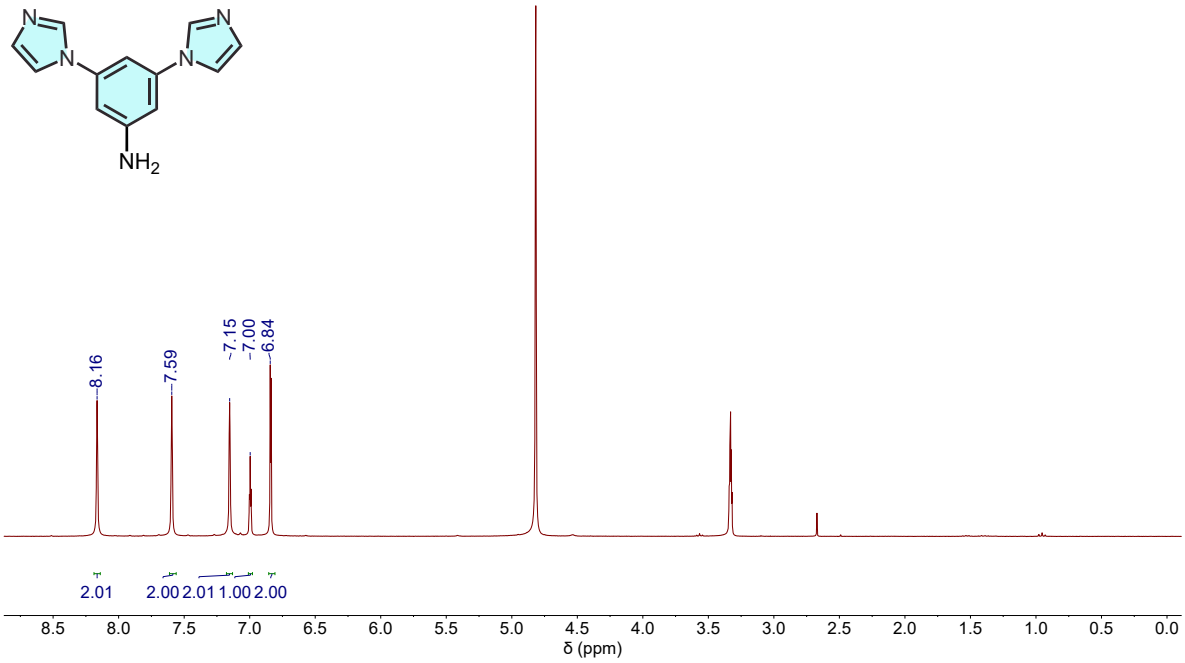

Figure S1. ^{1}H NMR spectrum (300 MHz, CD_3OD) of 3,5-bis(imidazol-1-yl)aniline

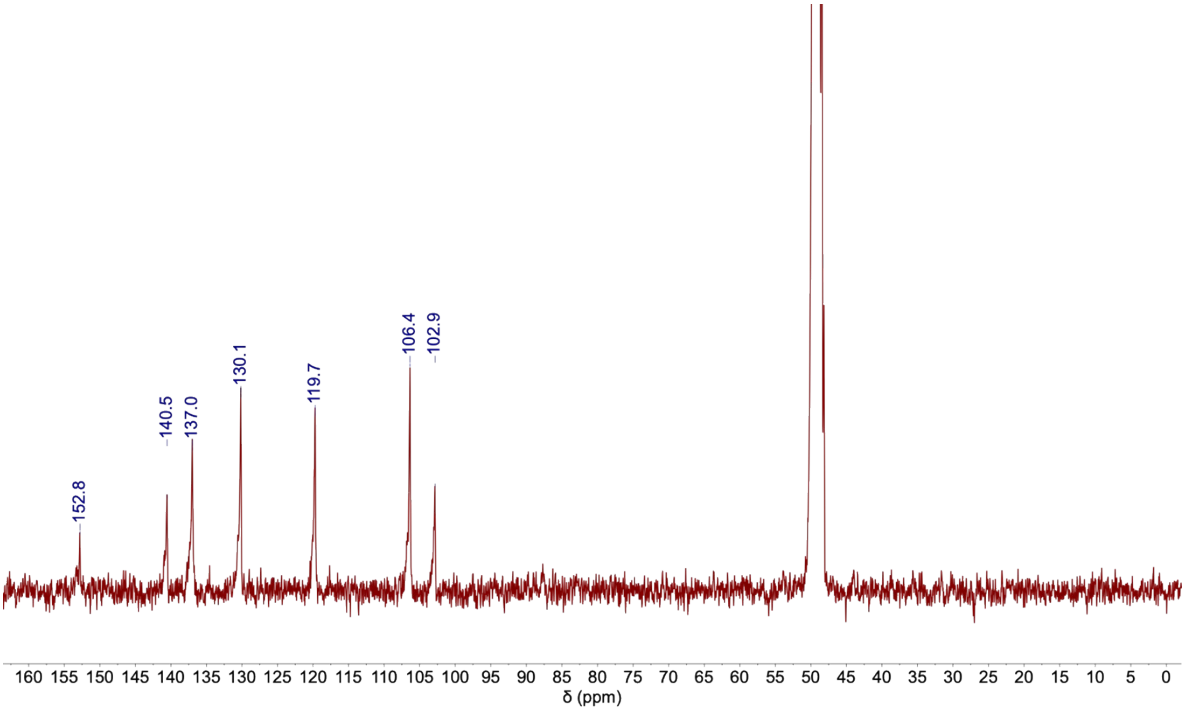

Figure S2. $^{13}C\{^{1}H\}$ NMR spectrum (75 MHz, CD_3OD) of 3,5-bis(imidazol-1-yl)aniline

2.2. ^{1}H and $^{13}C\{^{1}H\}$ NMR spectra of I

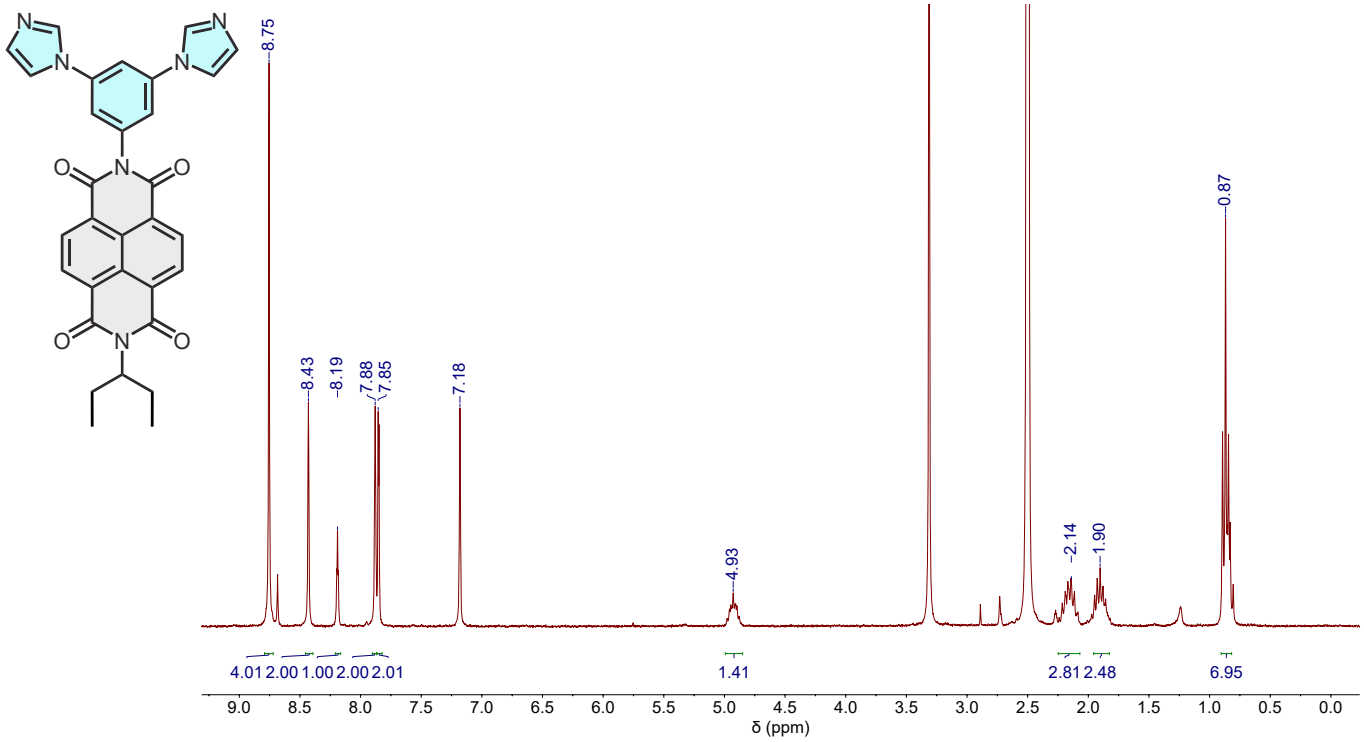

Figure S3. ^{1}H NMR spectrum (300 MHz, DMSO) of **I**

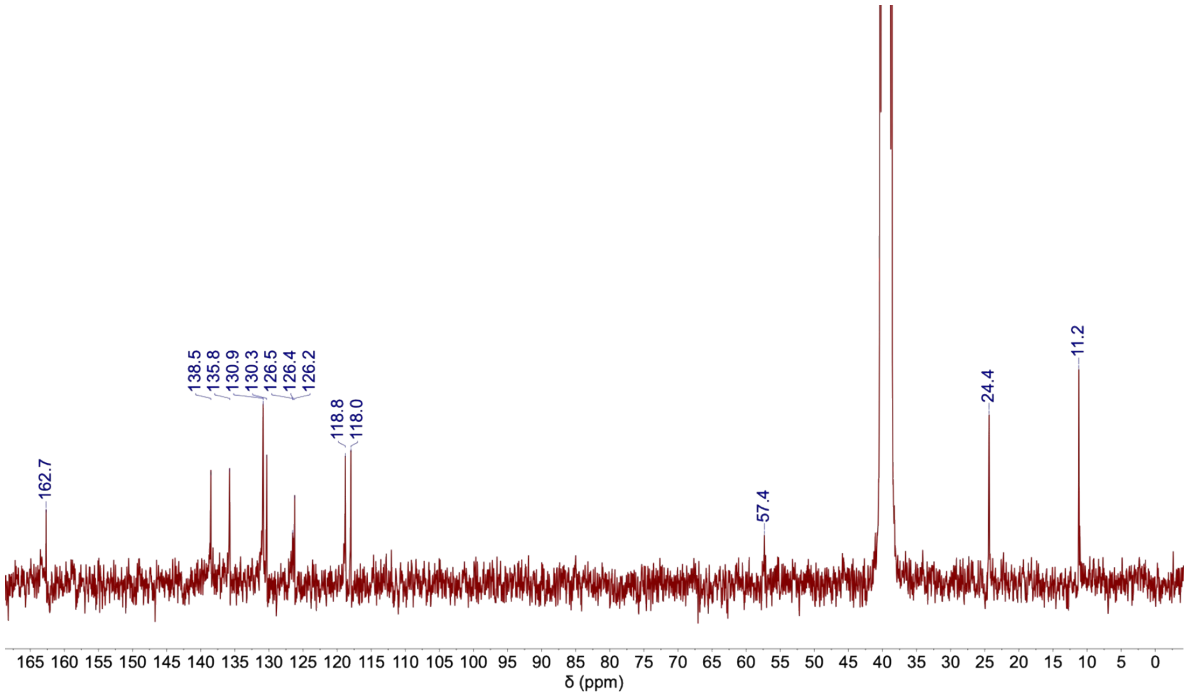

Figure S4. $^{13}C\{^{1}H\}$ NMR spectrum (75 MHz, DMSO) of **I**

2.3. ^{1}H and $^{13}C\{^{1}H\}$ NMR spectra of $[1](I)_2$

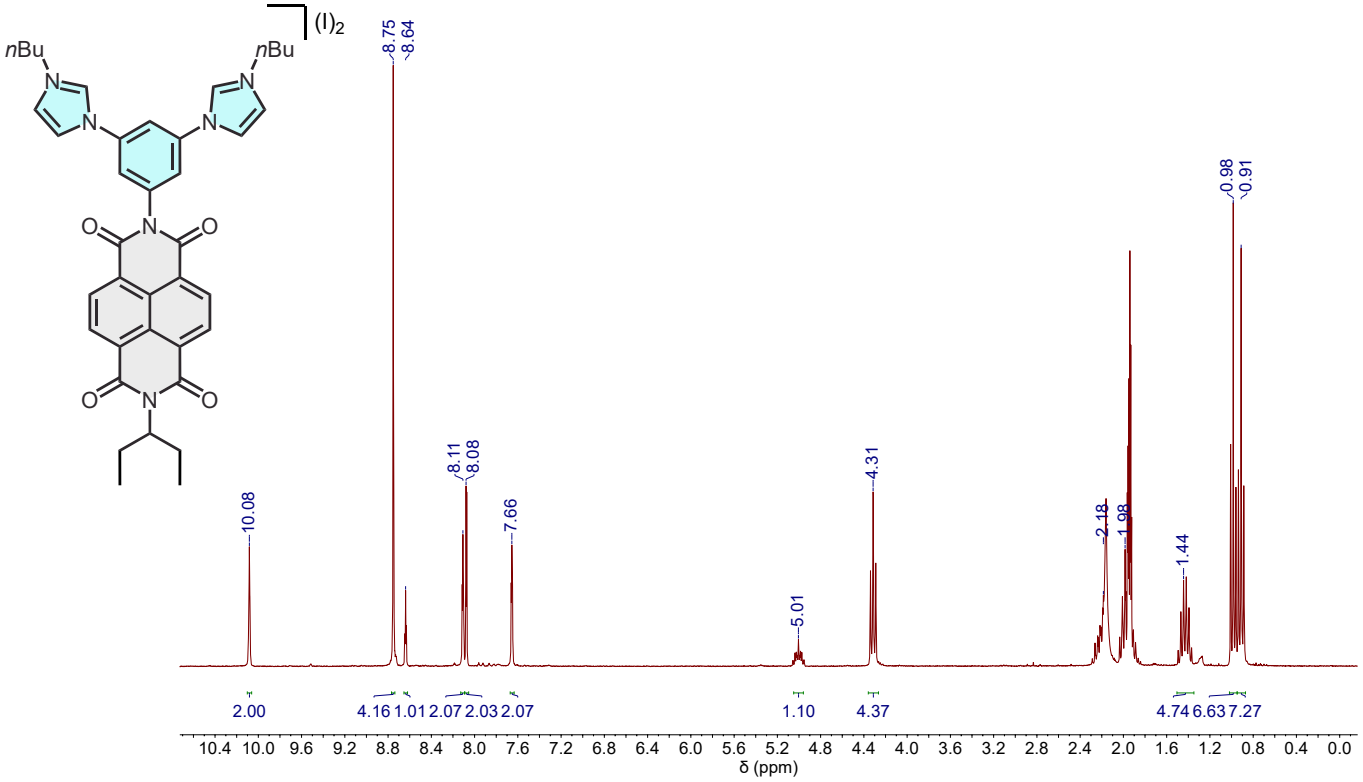

Figure S5. ^{1}H NMR spectrum (300 MHz, CD_3CN) of $[\mathbf{1}](I)_2$

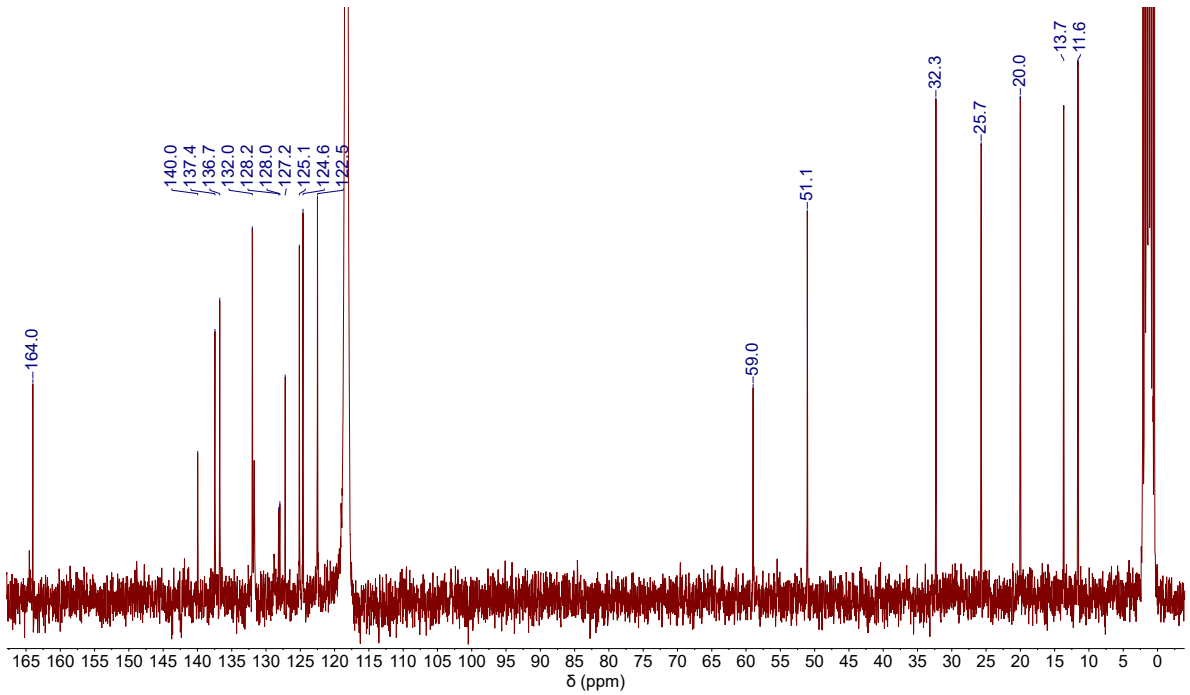

Figure S6. $^{13}C\{^{1}H\}$ NMR spectrum (75 MHz, CD_3CN) of $[\mathbf{1}](I)_2$

2.4. ^{1}H and $^{13}C\{^{1}H\}$ NMR spectra of 3,5-bis(imidazol-1-yl)toluene

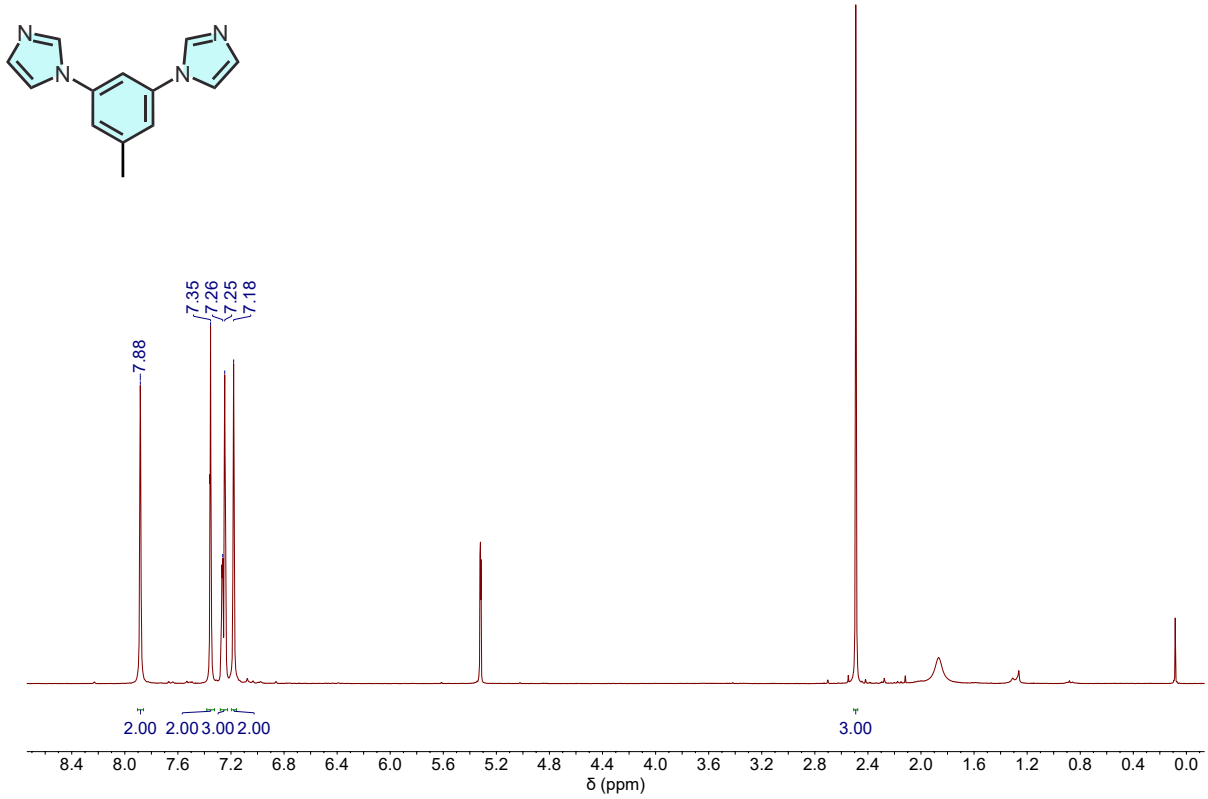

Figure S7. ^{1}H NMR spectrum (300 MHz, CD_2Cl_2) of 3,5-bis(imidazol-1-yl)toluene

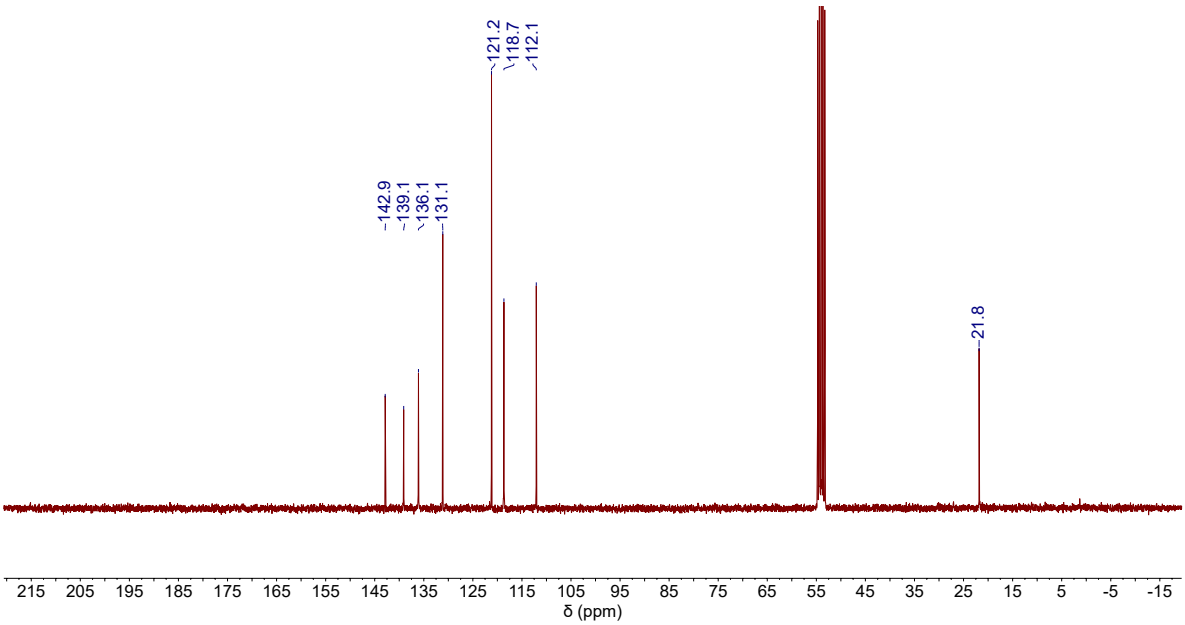

Figure S8. $^{13}C\{^{1}H\}$ spectrum (75 MHz, CD_2Cl_2) of 3,5-bis(imidazol-1-yl)toluene

2.5. ^{1}H and $^{13}C\{^{1}H\}$ NMR spectra of iodide salt $[2](I)_2$

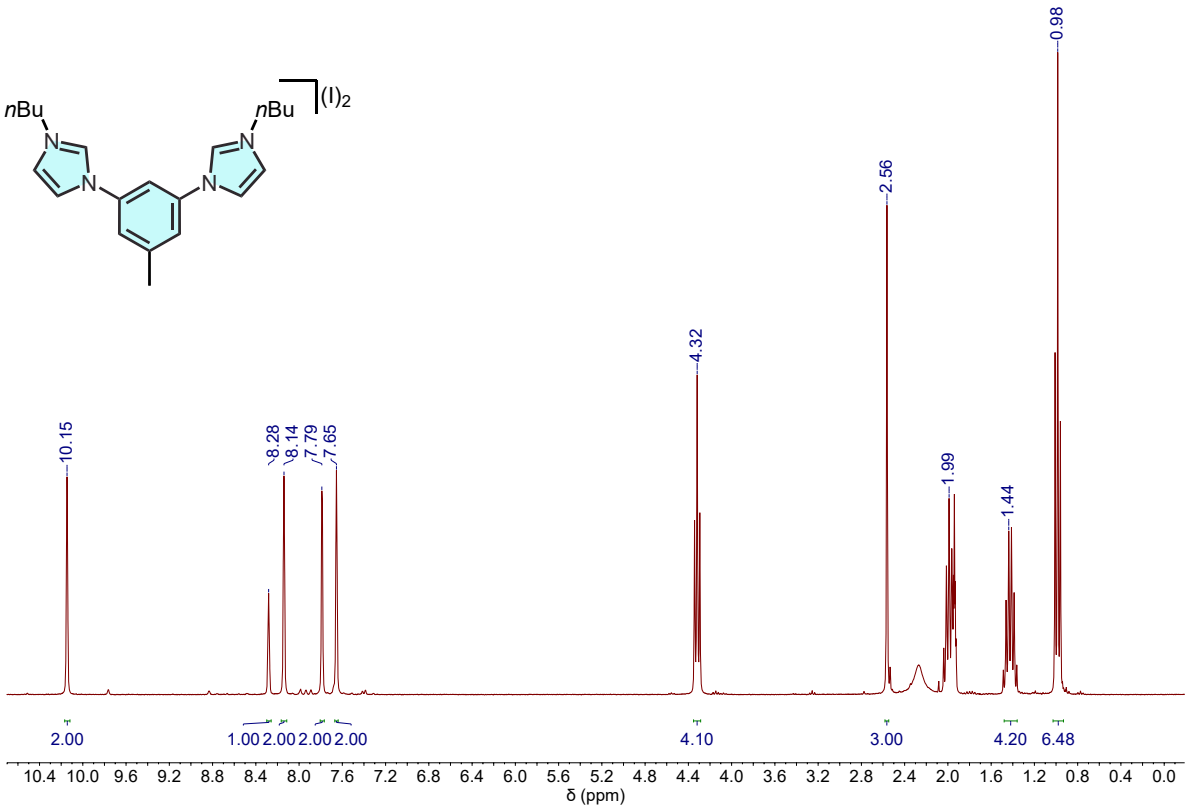

Figure S9. ^{1}H NMR spectrum (300 MHz, CD_3CN) of $[\mathbf{2}](I)_2$

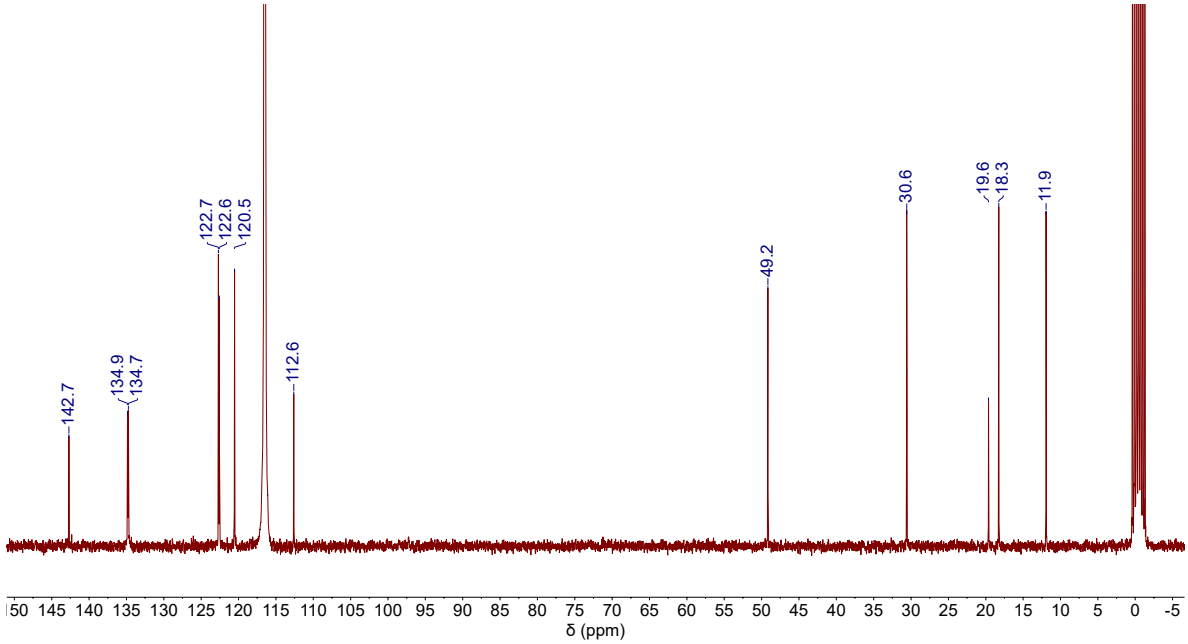

Figure S10. $^{13}C\{^{1}H\}$ spectrum (75 MHz, CD_3CN) of $[\mathbf{2}](I)_2$

2.6. ^{1}H and $^{13}C\{^{1}H\}$ NMR spectra of 4

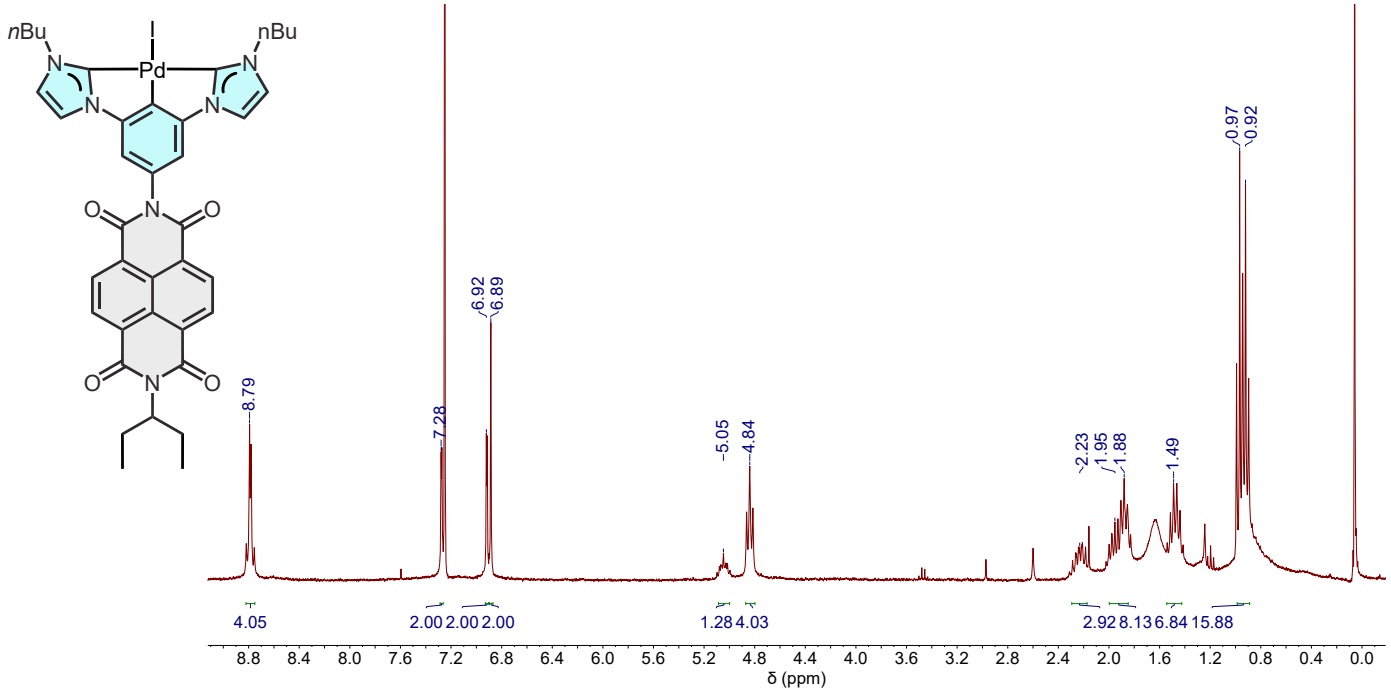

Figure S11. ^{1}H NMR spectrum (300 MHz, $CDCl_3$) of **4**

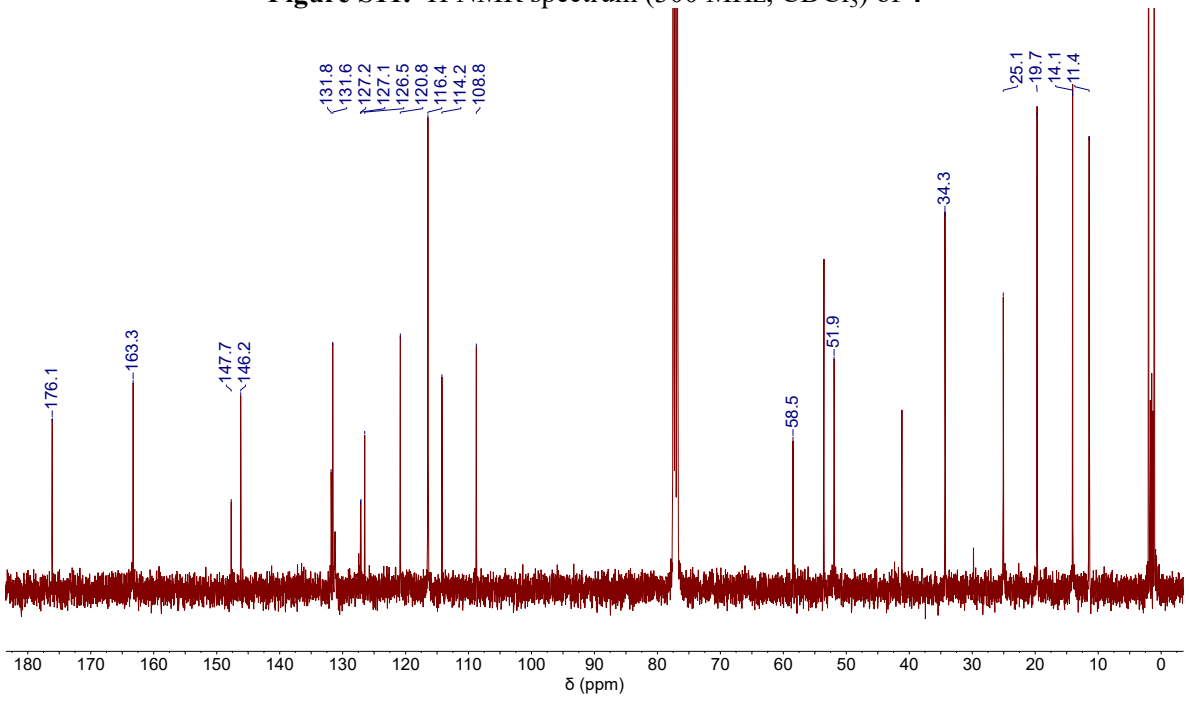

Figure S12. $^{13}C\{^{1}H\}$ spectrum (75 MHz, $CDCl_3$) of **4**

2.7. ^{1}H and $^{13}C\{^{1}H\}$ NMR spectra of 5

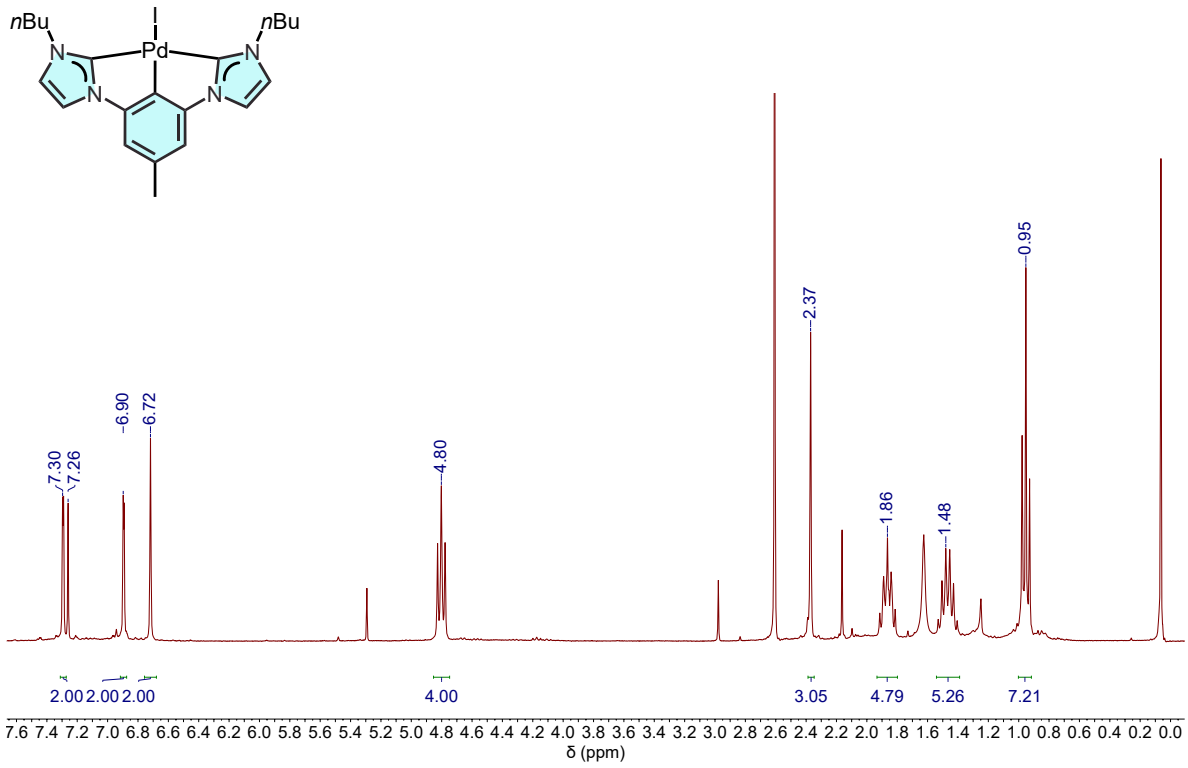

Figure S13. ^{1}H NMR spectrum (300 MHz, $CDCl_3$) of **5**

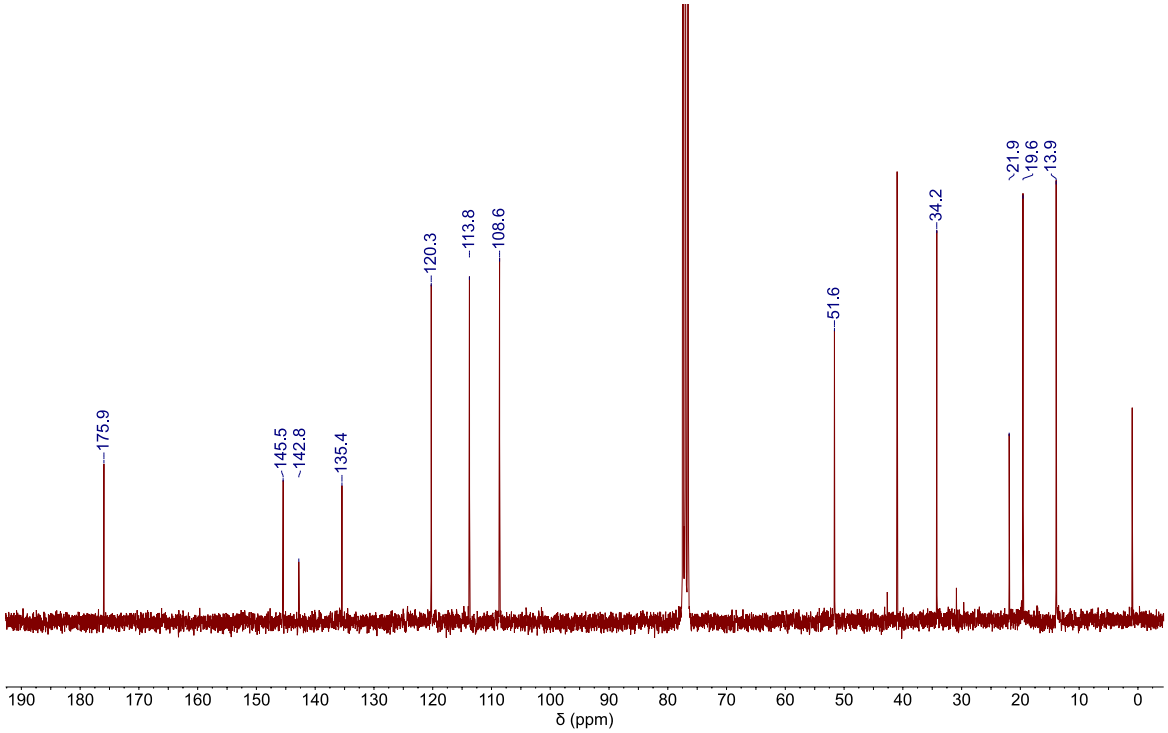

Figure S14. $^{13}C\{^{1}H\}$ spectrum (75 MHz, $CDCl_3$) of **5**

2.8. ^{1}H and $^{13}C\{^{1}H\}$ NMR spectra of 6

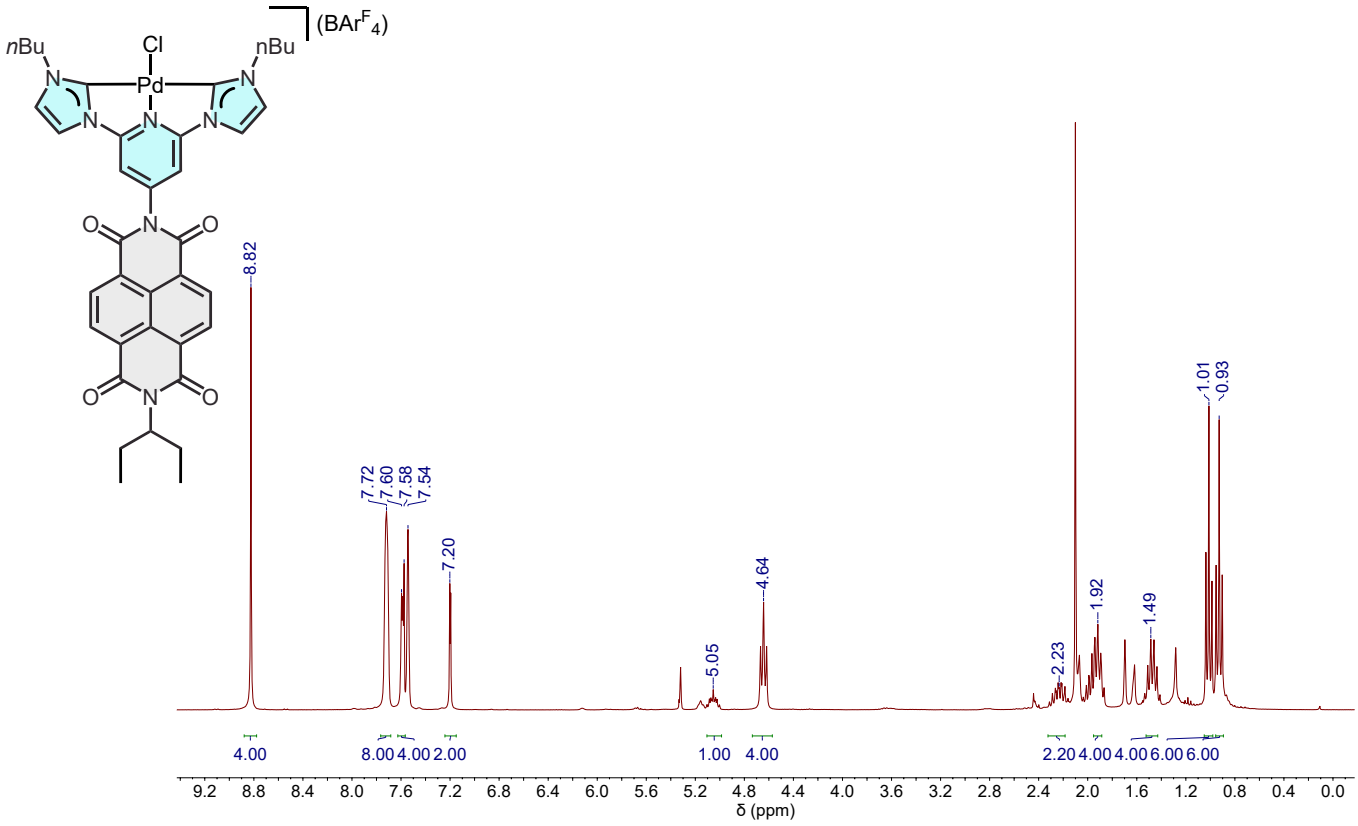

Figure S15. ^{1}H NMR spectrum (300 MHz, $CDCl_3$) of **6**

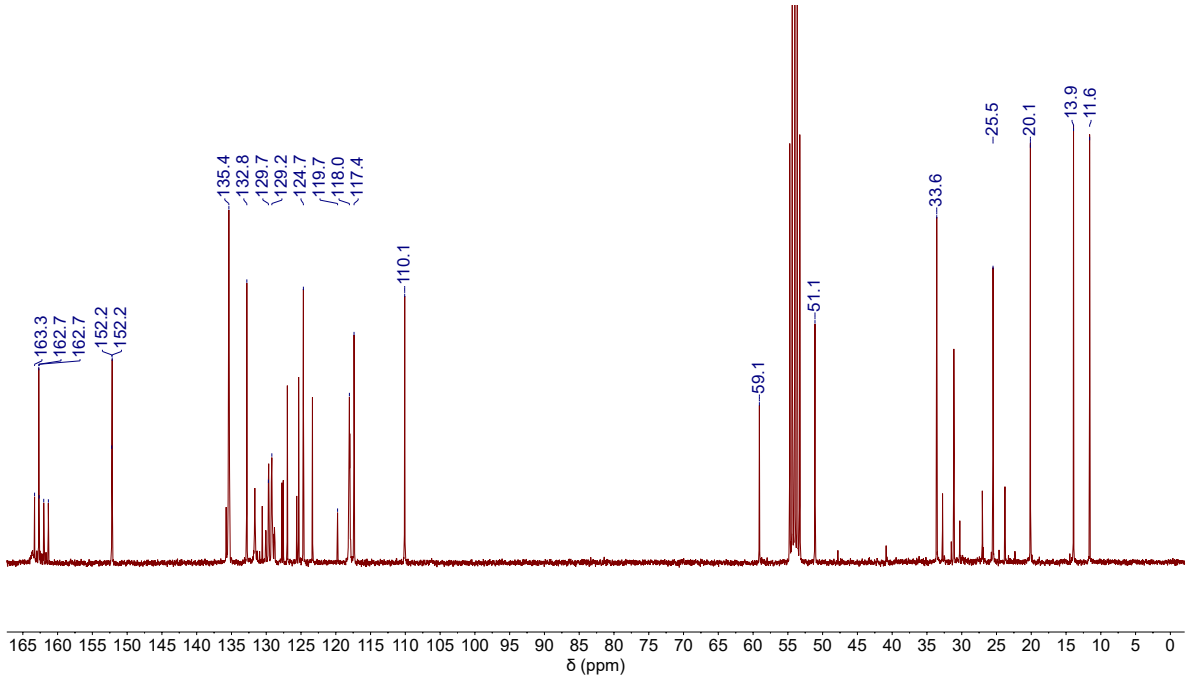

Figure S16. $^{13}C\{^{1}H\}$ spectrum (75 MHz, $CDCl_3$) of **6**

2.9. ^{1}H and $^{13}C\{^{1}H\}$ NMR spectra of 7

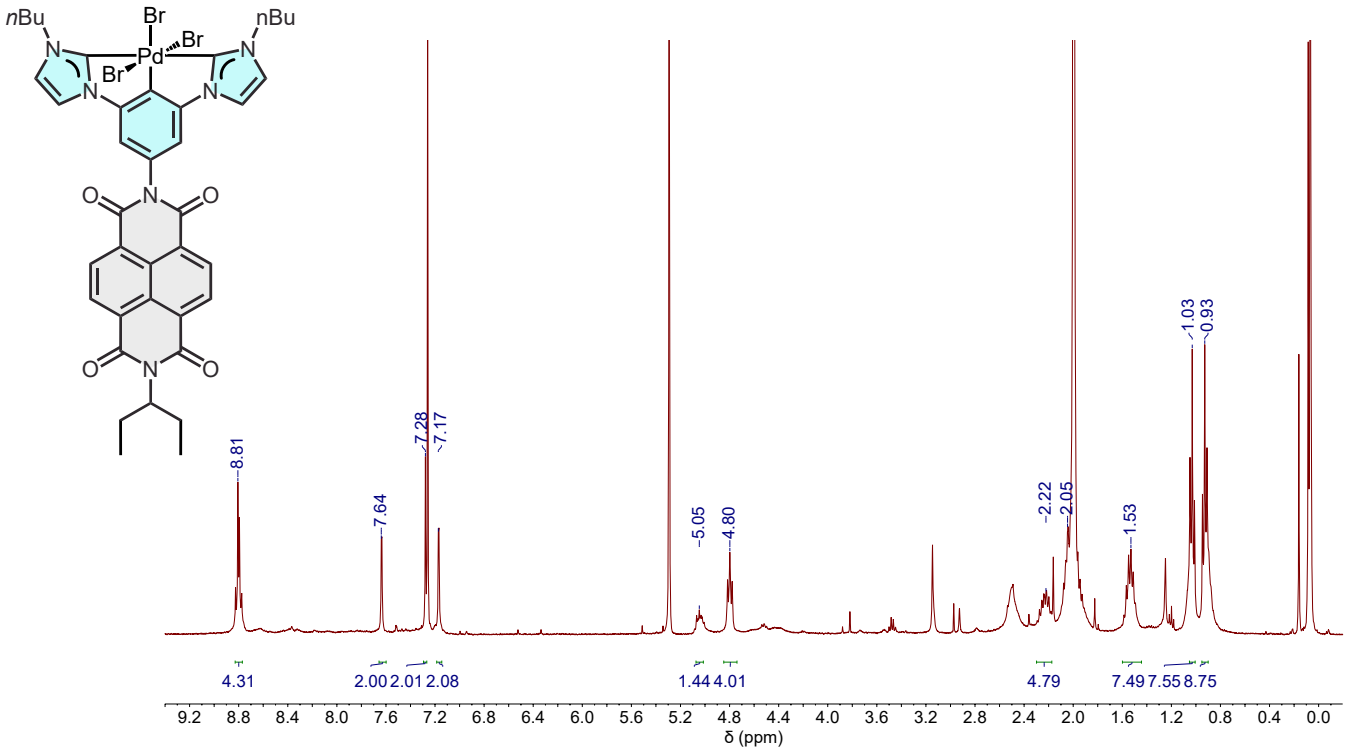

Figure S17. ^{1}H NMR spectrum (300 MHz, $CDCl_3$) of **7**

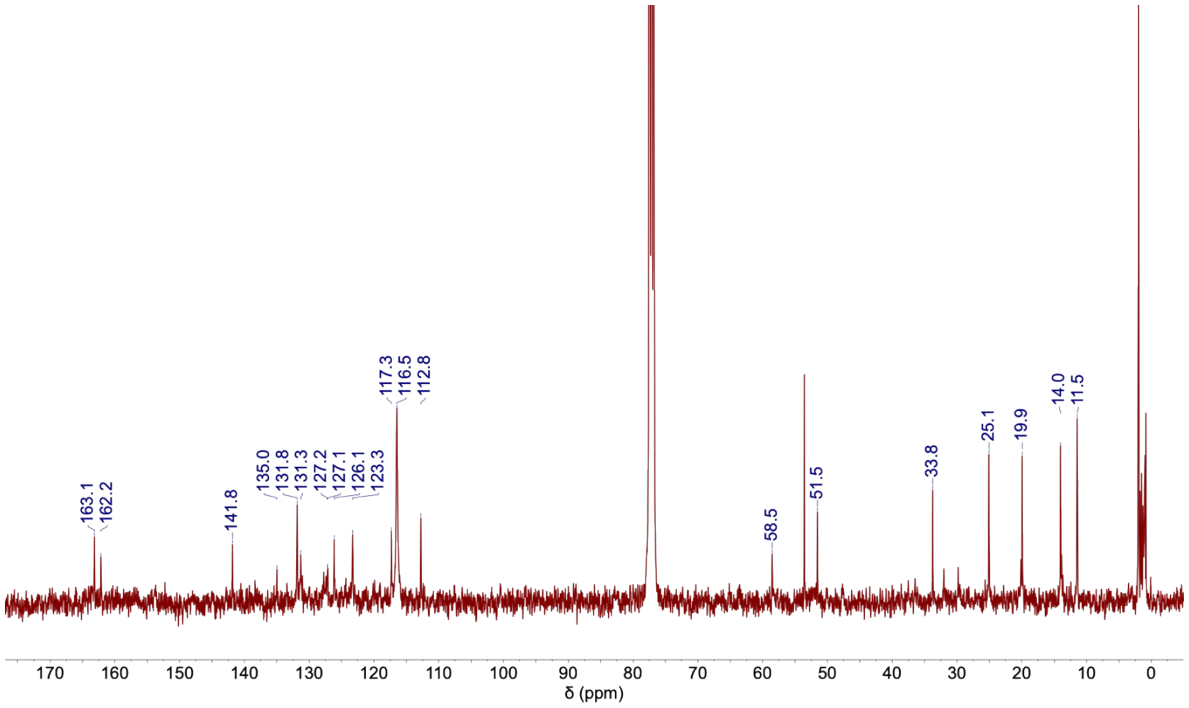

Figure S18. $^{13}C\{^{1}H\}$ spectrum (75 MHz, $CDCl_3$) of **7**

2.10. ^{1}H and $^{13}C\{^{1}H\}$ NMR spectra of 8

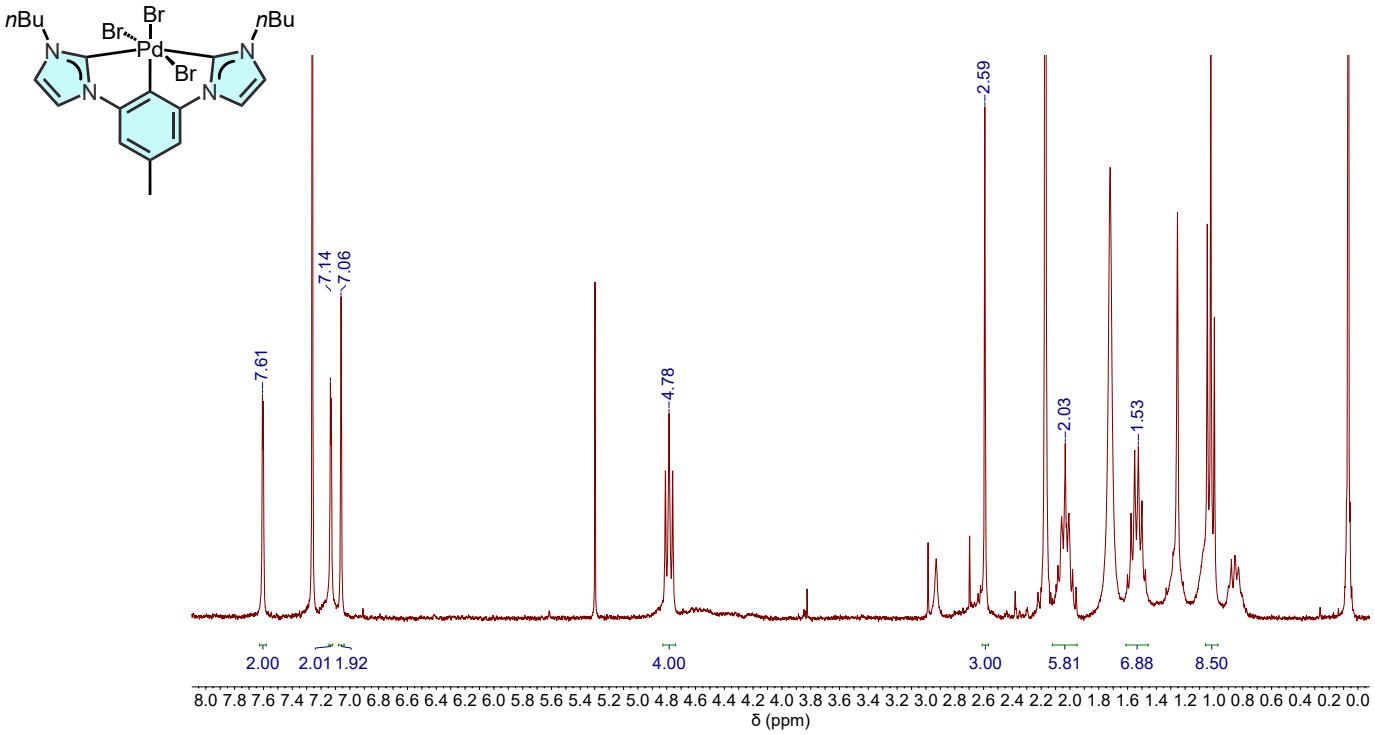

Figure S19. ^{1}H NMR spectrum (300 MHz, $CDCl_3$) of **8**

2.11. ^{1}H and $^{13}C\{^{1}H\}$ NMR spectra of 9

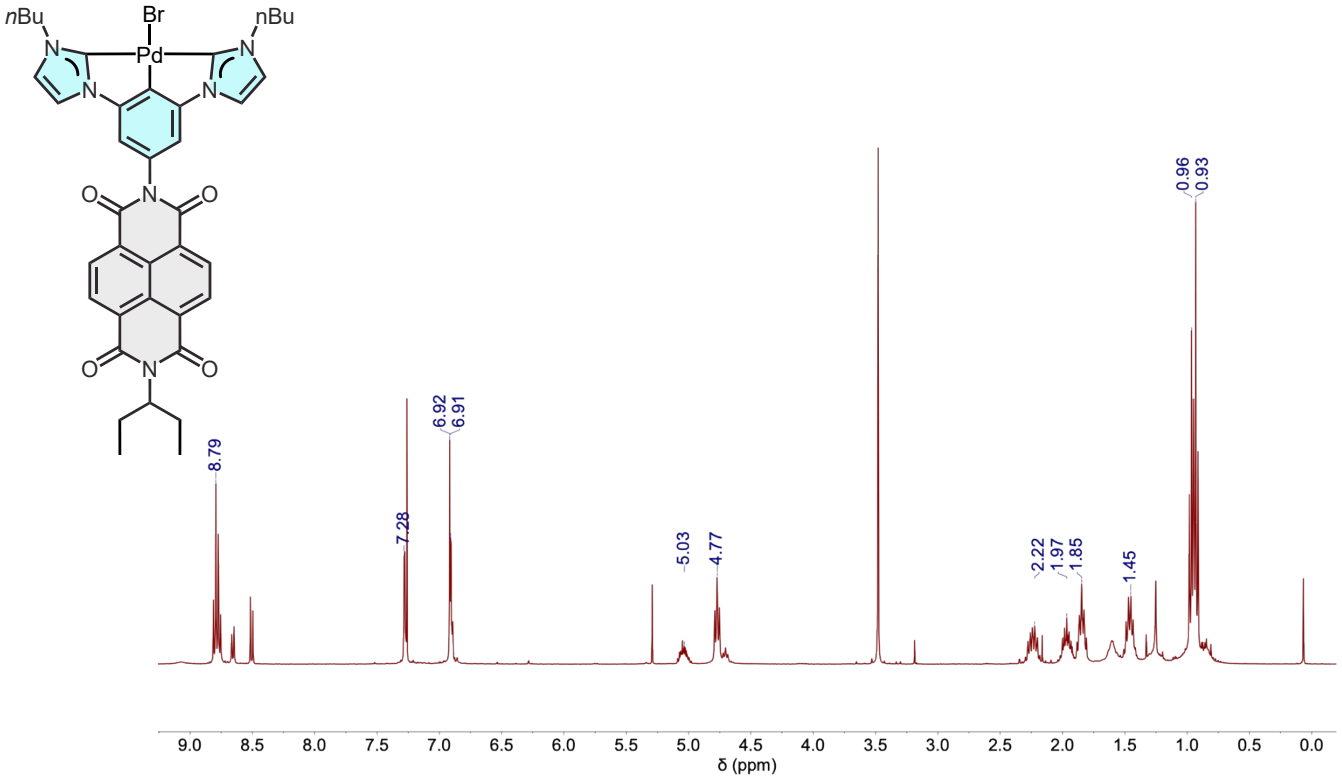

Figure S20. ^{1}H NMR spectrum (300 MHz, $CDCl_3$) of **9**

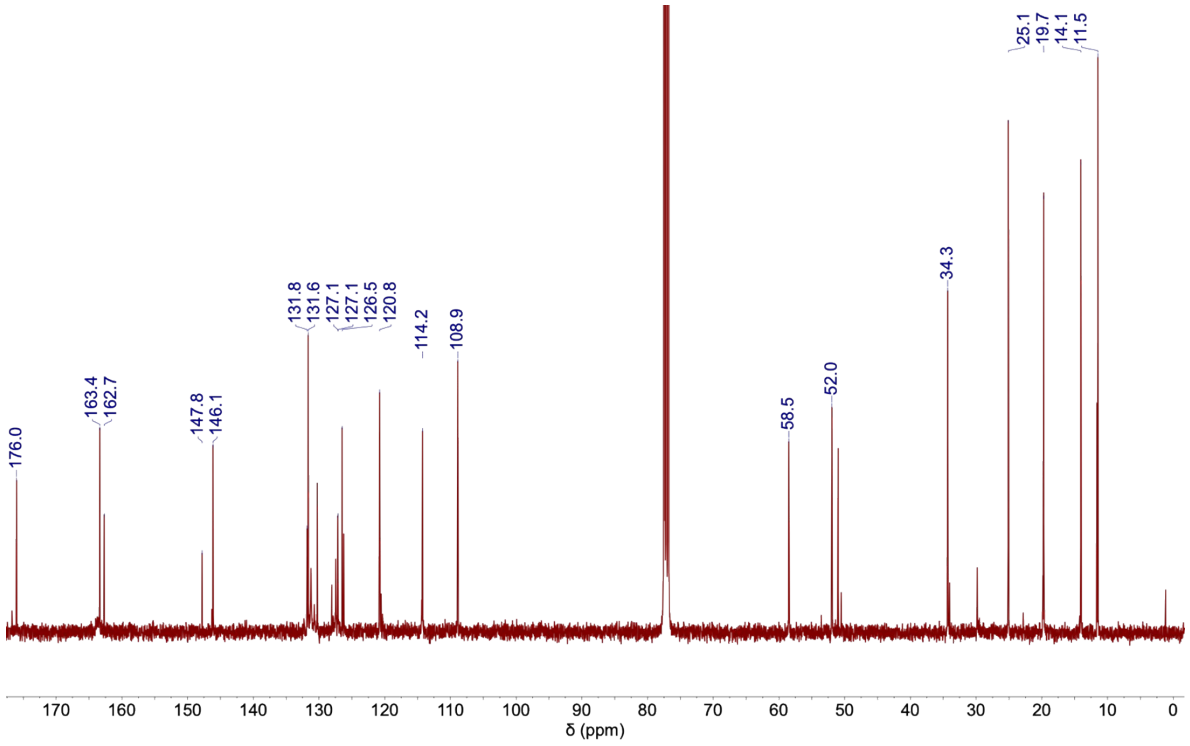

Figure S21. ^{1}H NMR spectrum (300 MHz, $CDCl_3$) of **9**

3. Photophysical properties

Pd(II) species

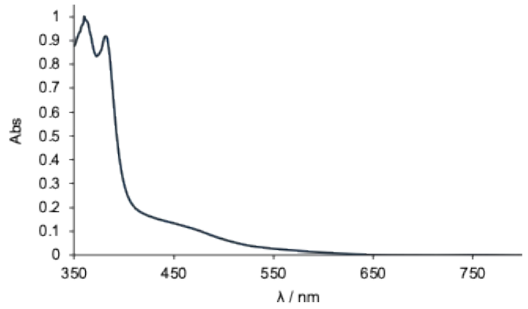

Figure S22. UV-Vis spectrum of NDI-containing complex **4**

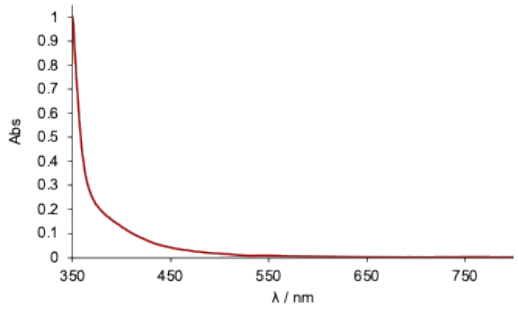

Figure S23. UV-Vis spectrum of complex **5**

Pd(IV) species

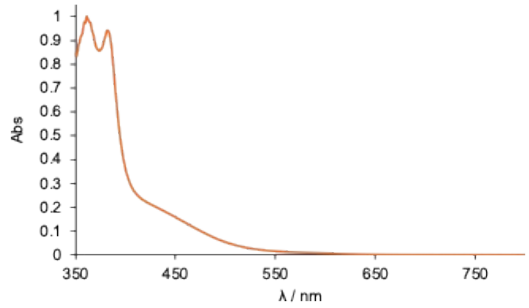

Figure S24. UV-Vis spectrum of NDI-containing complex **7**

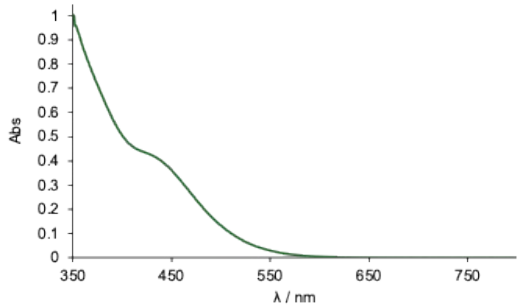

Figure S25. UV-Vis spectrum of complex **8**

4. X-Ray crystallography

General comments on the X-Ray Diffraction studies for compounds [1](I)$_2$, 6 and 7. Single crystals for X-Ray studies of [**1**](I)$_2$ were obtained by slow diffusion of diethyl ether into a solution of the compound in acetonitrile. Single crystals for X-Ray studies of complex **6** were obtained by slow diffusion of diethyl ether into a solution of the complex in dichloromethane. Single crystals for X-Ray studies of **7** were obtained by slow diffusion of pentane into a solution of the complex in dichloromethane.

The diffraction data for compound [**1**](I)$_2$ were collected on a Bruker D8 VENTURE diffractometer equipped with a PHOTON III-14 detector using a Mo Incoatec Microfocus Source IμS 3.0 (λ = 0.71073 Å). Absorption corrections based on multi-scan methods. The diffraction data for complexes **6** and **7** were collected on an Agilent SuperNova diffractometer equipped with an Atlas CCD detector using Cu-Kα radiation (λ = 1.54184 Å). Single crystals were mounted on a MicroMount® polymer tip (MiteGen) in a random orientation. Absorption corrections based on Gaussian methods.

Using Olex2,[3] the molecular structure of the compounds was solved by Charge Flipping in Superflip,[4] and refined by least squares with the ShelXL refinement package.[5] H-atoms were introduced in calculated positions and refined on a riding model. Non-hydrogen atoms were refined anisotropically. Key details of the crystals and structure refinement data are summarized in Supplementary Table S1. Further crystallographic details may be found in the CIF files, which were deposited at the Cambridge Crystallographic Data Centre, Cambridge, UK. The reference number for compounds [**1**](I)$_2$, **6** and **7** were assigned as 2387767, 2387900 and 2387768, respectively.

4.1. Molecular structure of [1](I)$_2$

The asymmetric unit contains two molecules of the compound. Figure S27 shows two different perspective views of the X-Ray molecular structure of [**1**](I)$_2$, which consists of a phenyl-bis-imidazolium salt that contains an NDI fragment at the 4-position of the phenyl ring. CheckCIF on Platon shows the following A alerts:

PLAT971_ALERT_2_A Check Calcd Resid. Dens. 0.85Ang From I3 4.19 eA-3
PLAT972_ALERT_2_A Check Calcd Resid. Dens. 0.72Ang From I3 -3.60 eA-3

RESPONSE: It is normal to expect the largest residual electron density to be associated with heavy atoms. While these are larger than expected residuals, the data was checked for signs of twinning, using PLATON, and no twin law was detected. Finally, given the proximity to the heavy atom, it is not likely that these peaks represent solvent, or other small molecules that have been missed.

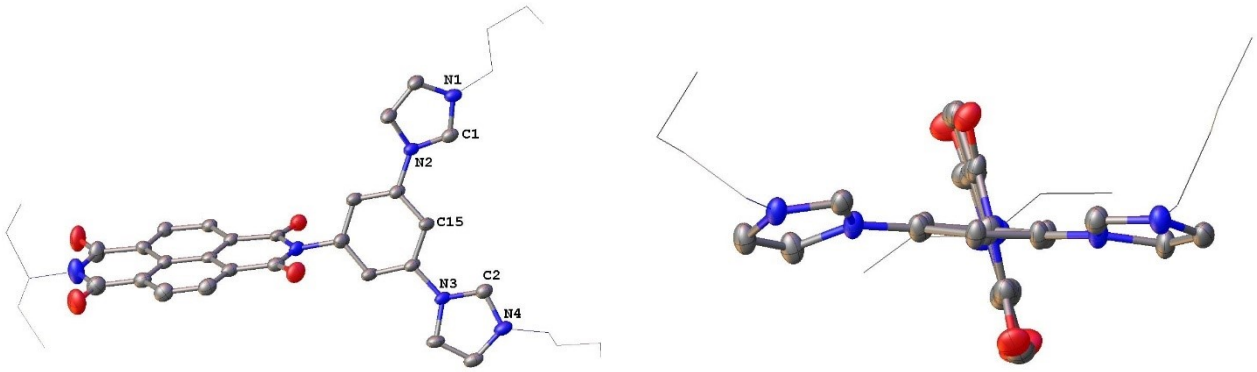

Figure S26. Different perspective views of the molecular structure of [**1**](I)$_2$. Hydrogen atoms and counter anions ($2I^-$) have been omitted for clarity. Alkyl chains are represented in the wireframe form. Ellipsoids at 50% probability. C grey, O red, N light blue

4.2. Molecular structure of 6

A global, enhanced rigid bond restraint (SHELX RIGU) was applied during the refinement of the structure model of **6**. CheckCIF on Platon does not show A alerts.

4.3. Molecular structure of 7

CheckCIF on Platon does not show A alerts.

Table S1. Summary of crystal data, data collection, and structure refinement details of compounds [**1**](I)$_2$, **6** and **7**.

	[**1**](I)$_2$	**6**	**7**
Empirical formula	$C_{39}H_{42}I_2N_6O_4$	$C_{70}H_{51}BClF_{24}N_7O_4Pd\cdot C_6H_4F_2$	$C_{39}H_{40}Br_3N_6O_4Pd\cdot CH_2Cl_2$
Formula weight	912.58	1776.93	1087.82
Temperature/K	100.00	200.00(14)	270(5)
Crystal system	triclinic	triclinic	monoclinic
Space group	P-1	P-1	$P2_1/c$
a/Å	14.2539(12)	13.7465(5)	11.0685(6)
b/Å	17.2346(16)	13.7475(5)	27.3218(10)
c/Å	17.3593(17)	21.0944(9)	14.8974(6)
α/°	106.528(3)	72.438(4)	90
β/°	102.260(3)	78.222(4)	110.129(5)
γ/°	90.213(3)	81.747(3)	90
Volume/Å^3	3985.7(6)	3706.3(3)	4230.0(3)
Z	4	2	4
ρ_{calc} g/cm^3	1.521	1.592	1.708
μ/mm^{-1}	1.624	3.439	8.412
F(000)	1824.0	1788.0	2164.0
Crystal size/mm^3	0.24 × 0.12 × 0.02	0.046 × 0.069 × 0.245	0.328 × 0.057 × 0.024
Radiation	Mo Kα	Cu Kα	Cu Kα
2Θ range for data collection/°	3.884 to 52.74	6.982 to 143.608	7.1 to 133.19
Index ranges	$-17 \le h \le 17$, $-21 \le k \le 21$, $-21 \le l \le 21$	$-16 \le h \le 11$, $-16 \le k \le 16$, $-25 \le l \le 25$	$-13 \le h \le 13$, $-24 \le k \le 32$, $-17 \le l \le 17$
Reflections collected	138674	39557	22366
Independent reflections	16285 [R_{int} = 0.0530, R_{sigma} = 0.0261]	14153 [R_{int} = 0.0875, R_{sigma} = 0.0866]	7471 [R_{int} = 0.0631, R_{sigma} = 0.0609]
Data/restraints/ parameters	16285/1/863	14153/983/1049	7471/475/454
Goodness-of-fit on F^2	1.088	1.032	1.040
Final R indexes [I>=2σ (I)]	R_1 = 0.0706, wR_2 = 0.1776	R_1 = 0.0799, wR_2 = 0.2072	R_1 = 0.0791, wR_2 = 0.2130
Final R indexes [all data]	R_1 = 0.0799, wR_2 = 0.1843	R_1 = 0.1109, wR_2 = 0.2370	R_1 = 0.1157, wR_2 = 0.2549
Largest diff. peak/hole / e Å^{-3}	4.18/-3.08	1.61/-1.45	1.27/-0.94

5. Electrochemical studies

5.1. Electrochemical measurements

Electrochemical studies were carried out by using an Autolab Potentiostat, Model PGSTAT101 controlled with NOVA 2.1.5 software. In all experiments, $[N(n\text{Bu})_4][PF_6]$ (0.25 M in dry CH_2Cl_2 and deoxygenated) was used as the supporting electrolyte, with an analyte concentration of 1 mM. In the particular case of [**1**]$(I)_2$, a 0.1 M solution of $[N(n\text{Bu})_4][PF_6]$ in dry and deoxygenated CH_3CN was used as the supporting electrolyte.

Cyclic voltammetry was performed in a cell, under Ar atmosphere and with disk glassy carbon working electrode, platinum counter electrode, and a silver wire pseudoreference electrode. Measurements were performed at 100 mVs^{-1} scan rate. All scans were referenced to the ferrocenium/ferrocene (Fc^+/Fc) couple at 0 V. Ohmic drop was minimized by minimizing the distance between the working and reference electrodes. The residual ohmic drop was estimated by positive feedback and compensated at 95%.

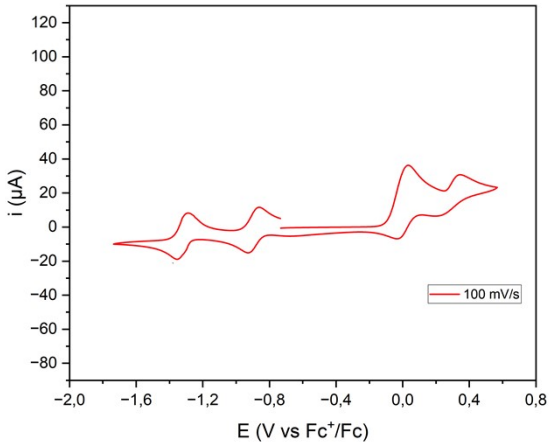

Figure S27. Cyclic voltammogram of [**1**]$(I)_2$ at 100 mV/s

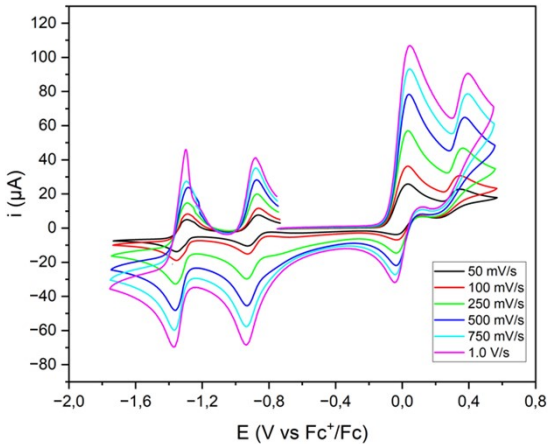

Figure S28. Cyclic voltammogram of [**1**]$(I)_2$ at different scan rates

Table S2. Electrochemical properties of complex [**1**]$(I)_2$

Ligand Precursor	$E_{1/2}$ (V)/ΔE (mV)	$E'_{1/2}$ (V)/ΔE (mV)
[**1**]$(I)_2$	-0.0.893/63	-1.1320/65

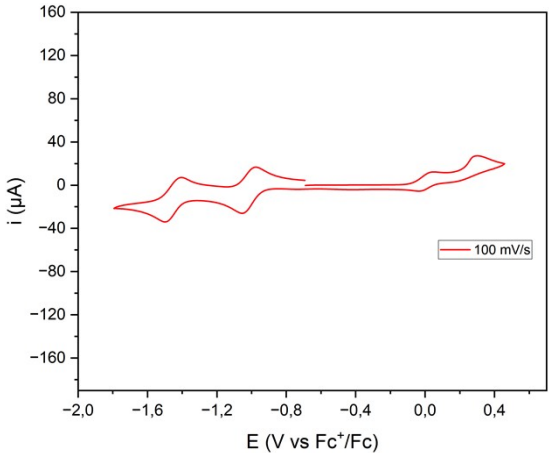

Figure S29. Cyclic voltammogram of **4** at 100 mV/s

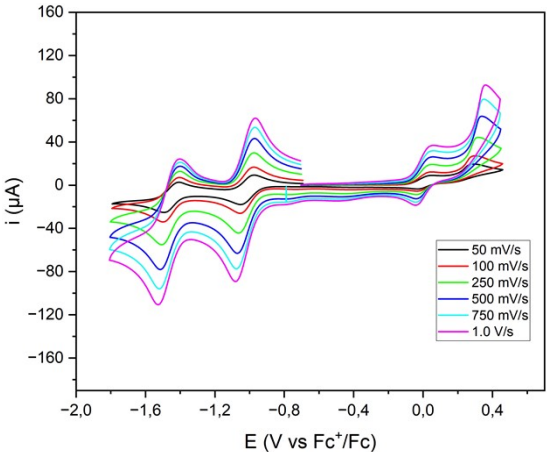

Figure S30. Cyclic voltammogram of **4** at different scan rates

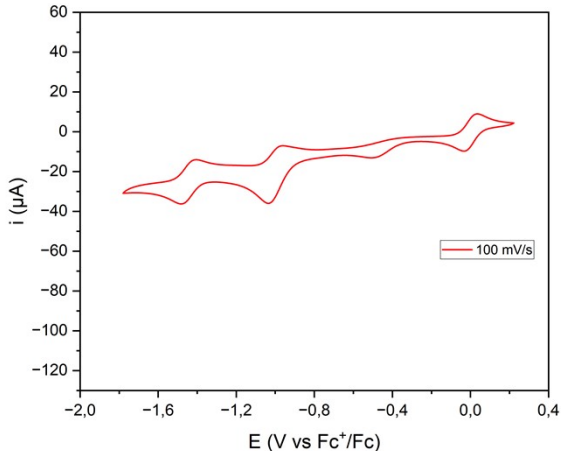

Figure S31. Cyclic voltammogram of **7** at 100 mV/s

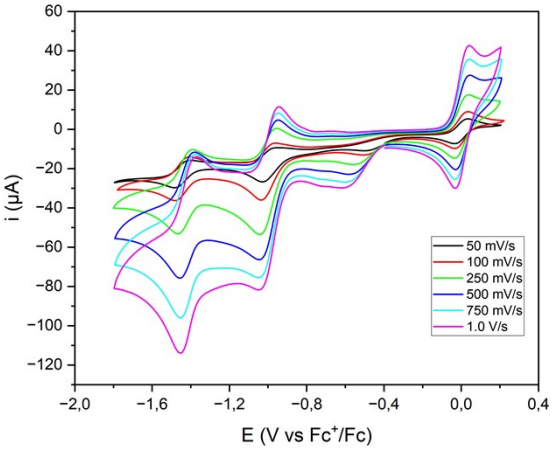

Figure S32. Cyclic voltammogram of **7** at different scan rates

Table S3. Electrochemical properties of NDI-containing complexes **4** and **7**

Complex	E_{pc} (V)	$E_{1/2}$ (V)/ΔE (mV)	$E'_{1/2}$ (V)/ΔE (mV)	E_{pa} (V)
4	-	-1.0156/75	-1.4530/93	0.301
7	-0.502	-1.0007/61	-1.4450/65	-

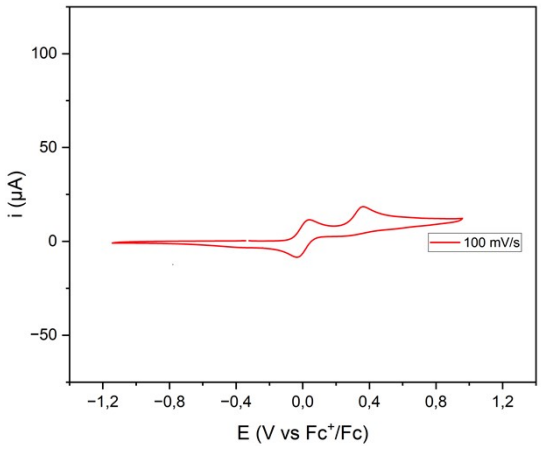

Figure S33. Cyclic voltammogram of **5** at 100 mV/s

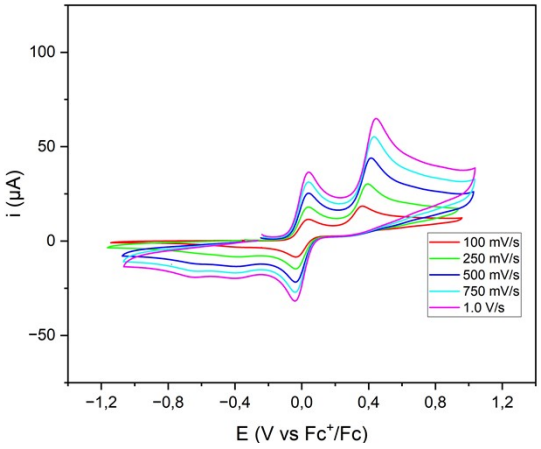

Figure S34. Cyclic voltammogram of **5** at different scan rates

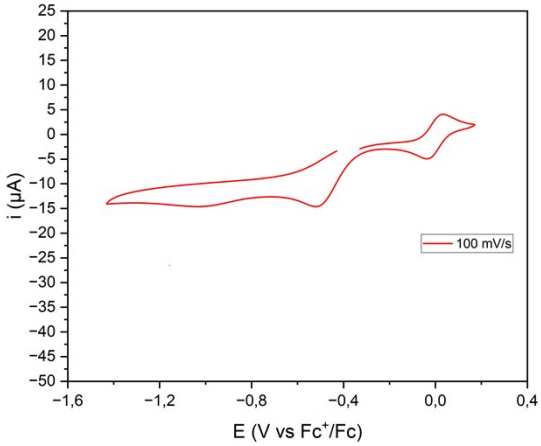

Figure S35. Cyclic voltammogram of **8** at 100 mV/s

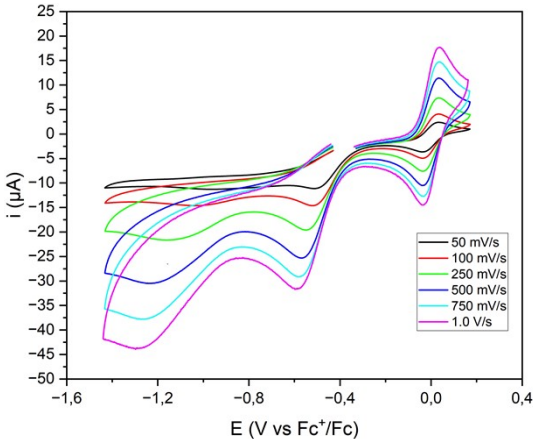

Figure S36. Cyclic voltammogram of **8** at different scan rates

Table S4. Electrochemical properties of non-NDI-containing complexes **5** and **8**

Complex	E_{pa} (V)	E_{pc} (V)
5	0.362	-
8	-	-0.494

5.2. UV-vis spectroelectrochemical studies

Spectroelectrochemical (SEC) measurements were performed using a gastight, optically transparent thin-layer solution cell fabricated by Prof. Hartl at the University of Reading (Reading, U.K.), as described previously.[6] The SEC cell contained a masked Au-minigrid working electrode (32 wires/cm), a Pt-gauze auxiliary electrode and an Ag-wire pseudo-reference electrode and had CaF_2 windows. In each experiment, electrochemical reduction of the species of interest ([**4**] = 1 mM, $[N(n\text{Bu})_4][PF_6]$ = 0.1 M in DMSO) was monitored by UV-vis spectroscopy for a period of 2−5 min. First, the potential of the cell was swept negatively starting at the open circuit potential, recording a thin-layer cyclic voltammogram (5 mV/s) to identify the potential window of interest. Then, fresh analyte solution was introduced in the cell and the potential was varied within range of interest in 33 mV steps. The electrolysis step did not exceed 30 s. After each step an UV-vis spectrum was collected. Diffusion and mixing of the redox products generated at the working and auxiliary electrodes in the cell were reasonably suppressed within the total experimental time (no more than 5 min for one complete measurement). The UV-Vis-SEC monitoring reduction of complex **4** is shown in Figure 4a of the manuscript.

6. Study of the reactivity of Pd(II) complex 4

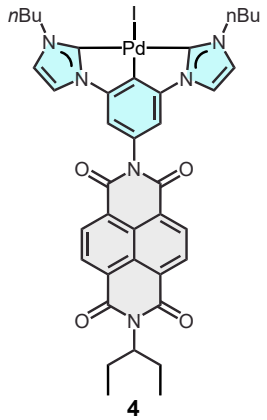

4

6.1. Study of the interaction with fluoride by UV-vis

The effect of the addition of fluoride to complex **4** was studied by means of a UV-visible titration experiment, by adding increasing amounts of TBAF·3H_2O (from 1 to 10 equivalents) to a solution of complex **4**. The experiment was conducted in dry DMSO, with complex **4** at an initial 5x10^{-5} M concentration (solution A) and TBAF·3H_2O at a 0.025 M concentration (solution B). The gradual addition of solution B to solution A resulted in changes in the absorption spectra of complex **4**. The UV-Vis spectroscopic changes in the spectrum of complex **4** upon the addition of TBAF·3H_2O is shown in Figure 4b of the manuscript.

6.2. Study of the interaction with fluoride by ^{1}H NMR

The interaction with fluoride of **4** and the reversibility of this process were studied by means of ^{1}H NMR spectroscopy, by sequentially adding TBAF·3H_2O and $NOBF_4$ to a solution of **4** in DMSO-d_6. An NMR tube was charged with 0.5 mL of a DMSO-d_6 solution of **4** (30.0 mM). Then, 100 µL of a TBAF·3H_2O solution in DMSO-d_6 (0.75 M, 5 equiv.) were added. As expected for the formation of a paramagnetic species, all the resonances due to the NDI-NHC ligand disappeared at this point (Figure S37b). Subsequent addition of 100 µL of a $NOBF_4$ solution (0.45 M, 3 equiv.) resulted in the recovery of complex **4** (Figure S37c).

6.3. Study of the interaction with hydroxide by ^{1}H NMR

^{1}H NMR experiments were performed to determine the effect of the addition of hydroxide (TBAOH·30 H_2O) on the resonances of the starting complex **4**. An NMR tube was charged with 0.5 mL of a DMSO-d_6 solution of complex **4** (30.0 mM). The addition of increasing volumes of a solution of TBAOH·30 H_2O in DMSO-d_6, resulted in a progressive disappearance of the resonances due to the protons of the NDI-NHC ligand, thus indicating the formation of a paramagnetic species (Figure S38).

6.4. Study of the interaction with cobaltocene by ^{1}H NMR

Cobaltocene (2.2 mg, 1 equiv.) was added as a solid to an NMR tube charged with 0.5 mL of a DMSO-d_6 solution of complex **4** (15.0 mM). As can be seen in Figure S39b, upon the addition of 1 equivalent of cobaltocene, resulted in the formation of the paramagnetic species $\mathbf{9}^{\bullet-}$.

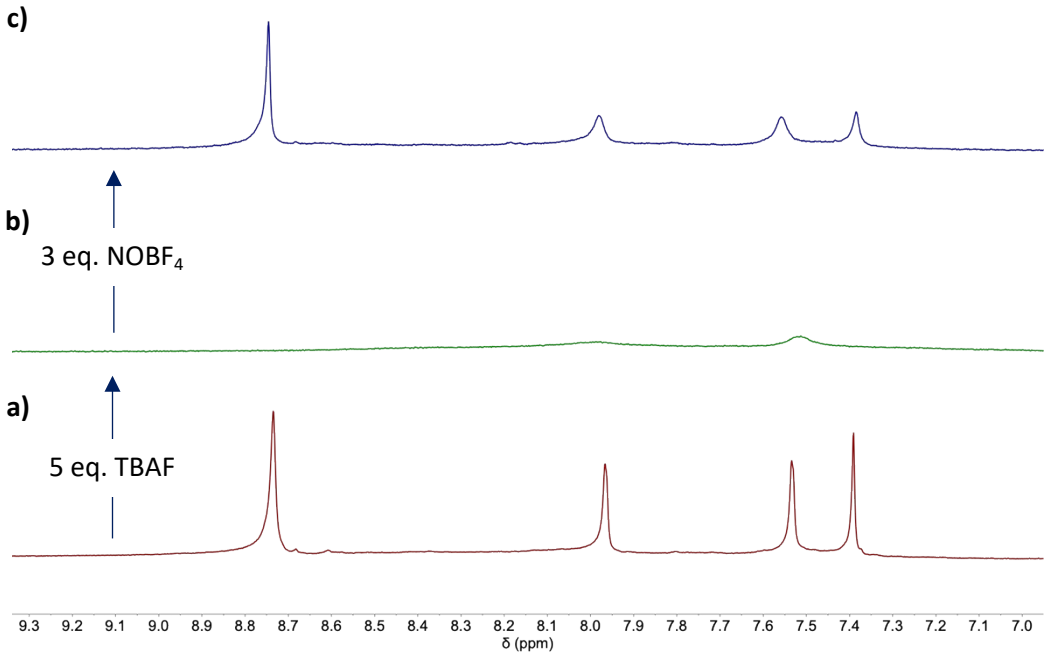

Figure S37. Selected region of the ^{1}H NMR spectra of **4** (300 MHz, DMSO-d_6, 298 K) (red), upon the addition of 5 equiv. of TBAF·3H_2O (green) and upon the addition of 5 equiv. of $NOBF_4$ (blue).

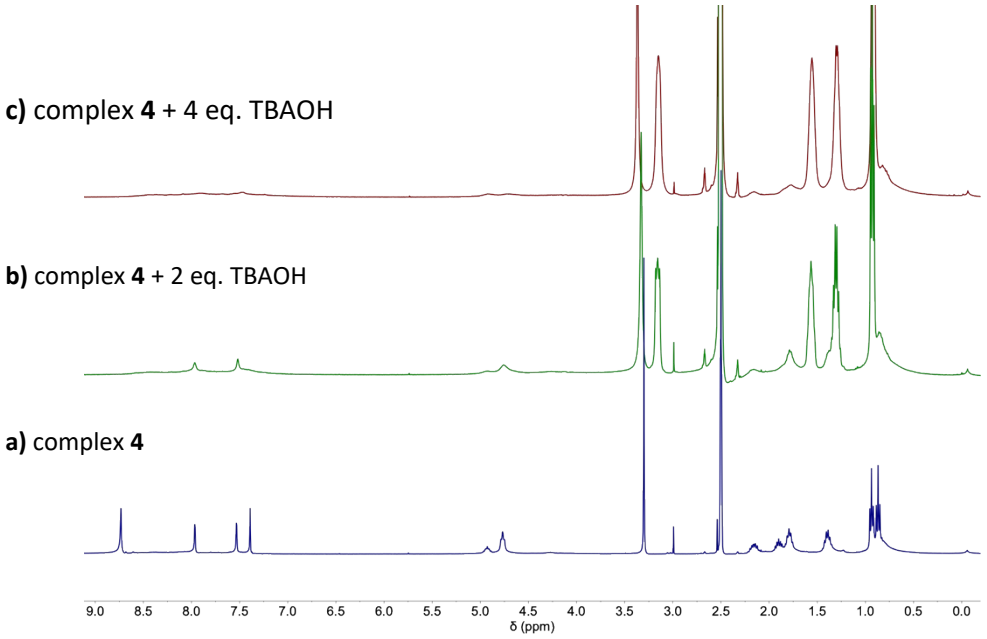

Figure S38. Selected region of the ^{1}H NMR spectra (300 MHz, DMSO-d_6, 298 K) of **4** upon the addition of increasing amounts of TBAOH·30H_2O

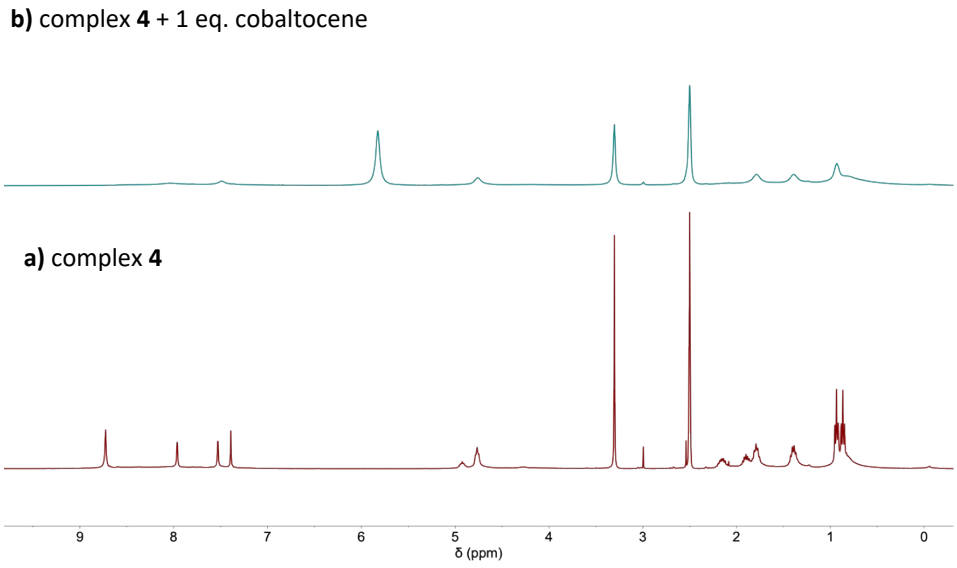

Figure S39. Selected region of the ^{1}H NMR spectra (300 MHz, DMSO-d_6, 298 K) of **4** upon the addition of 1 eq. of cobaltocene

7. Study of the reactivity of Pd(IV) complexes 7 and 8

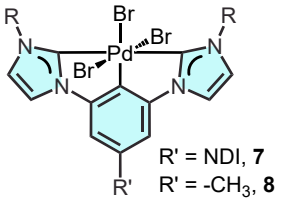

7.1. Study of the interaction with fluoride by ^{1}H NMR

^{1}H NMR experiments were performed to determine the effect of the addition of fluoride (TBAF·3H$_2$O) on the resonances of the starting complexes **7** and **8**. An NMR tube was charged with 0.8 mL of a DMSO-d_6 solution of the corresponding complex (16.0 mM).

- **Interaction of complex 7 with fluoride.** In the case of complex **7**, the addition of increasing volumes of a solution of TBAF·3H$_2$O in DMSO-d_6, first resulted in the formation of its Pd(II) counterpart **9** (Figure S40d) and eventually in the formation of the paramagnetic species **9**$^{\bullet-}$ (Figure S40e).

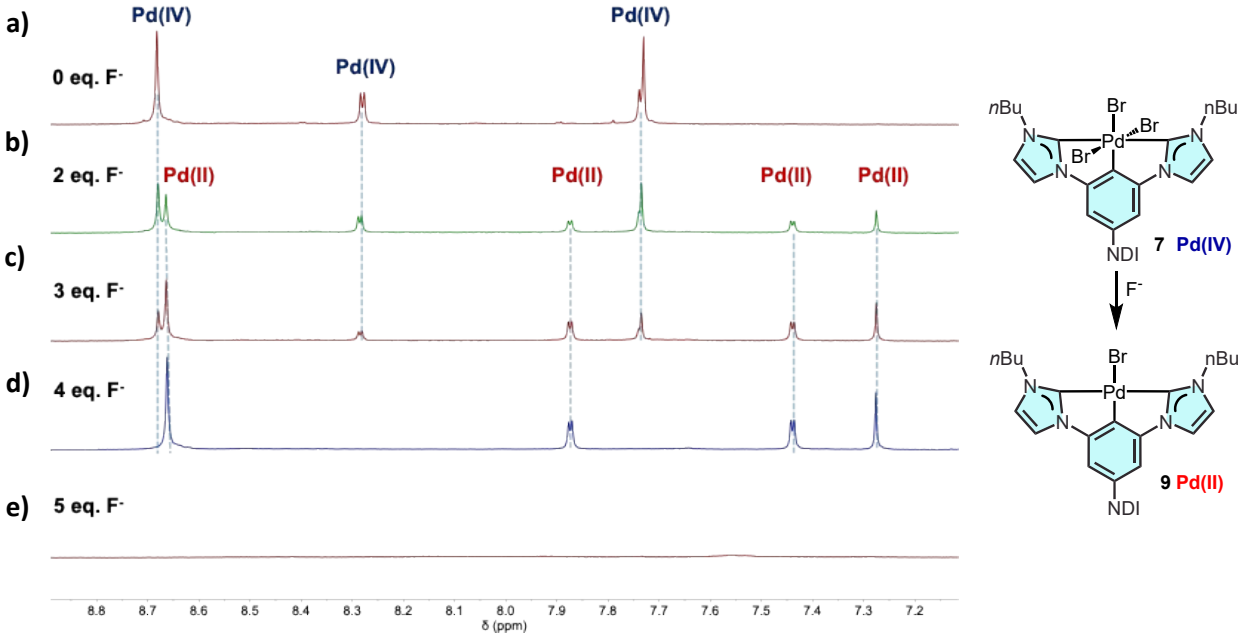

Figure S40. Selected region of the ^{1}H NMR spectra of complex **7** in DMSO-d_6 (a) upon the addition of increasing amounts of TBAF·3H$_2$O showing the formation of its Pd(II) counterpart (b-d) and a paramagnetic species (e)

- **Interaction of complex 8 with fluoride.** In the case of complex **8**, no changes in the resonances were observed upon the addition of fluoride as can be seen in Figure S41.

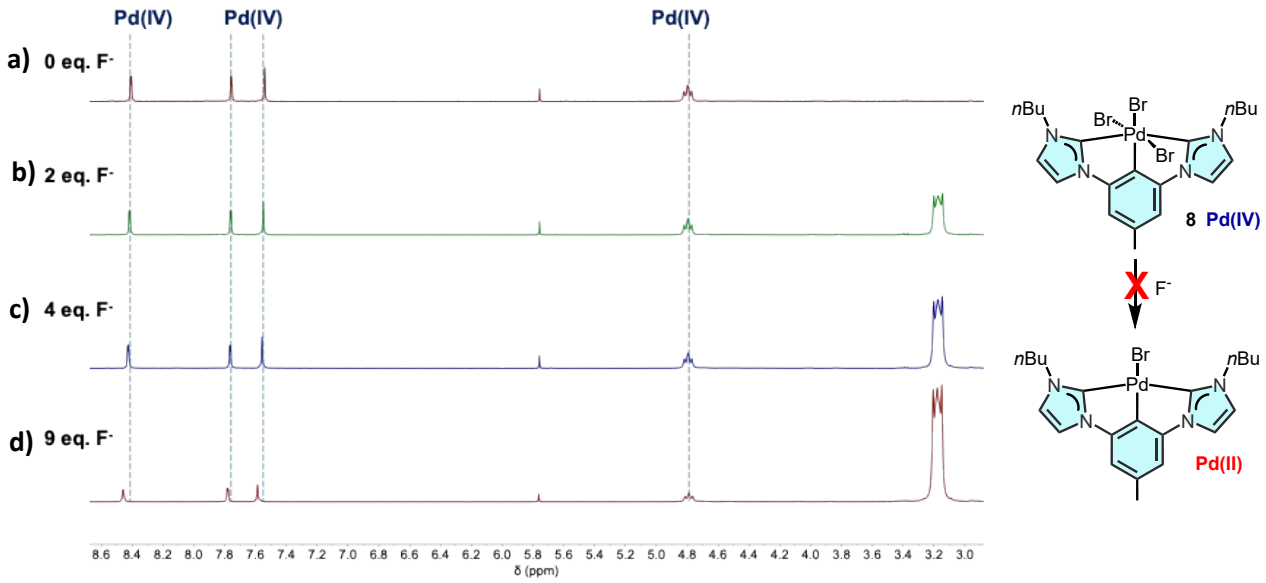

Figure S41. Selected region of the ^{1}H NMR spectra of complex **8** in DMSO-d_6 (a) upon the addition of increasing amounts of TBAF·3H_2O

- **Interaction of complex 8 and N,N'-di-(1-ethylpropyl)-1,4,5,8-naphthalenetetracarboxylic-diimide with fluoride.** We dissolved complex **8** and N,N'-di-(1-ethylpropyl)-1,4,5,8-naphthalenetetracarboxylic-diimide (NDI) in DMSO-d_6 and added 4 equivalents of TBAF·3H_2O.

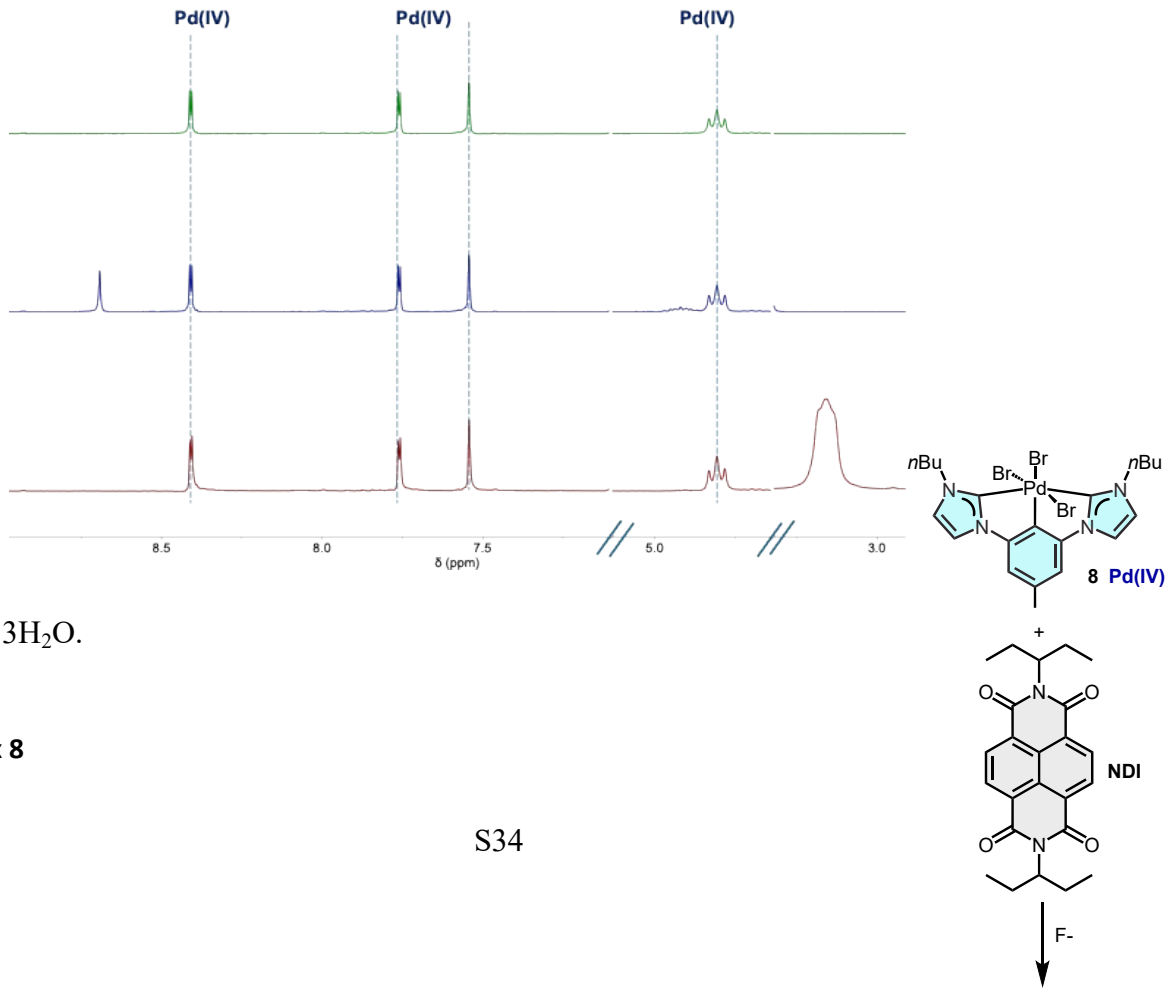

a) complex **8**

b) complex **8**
+ NDI

c) complex **8**
+ NDI + TBAF

Figure S42. Selected region of the ^{1}H NMR spectra of complex **8** (a) in the presence of NDI in DMSO-d_6 (b) and upon the addition of increasing amounts of 4 equivalents of TBAF·3H_2O (c)

7.2. Study of the interaction with cobaltocene by ^{1}H NMR

Cobaltocene (4.4 mg, 2 equiv.) was added as a solid to an NMR tube charged with 0.5 mL of a DMSO-d_6 solution of complex **8** (14.6 mM). As can be seen in Figure S43, the addition of 2 equivalents of cobaltocene resulted in the reduction of Pd(IV) to Pd(II).

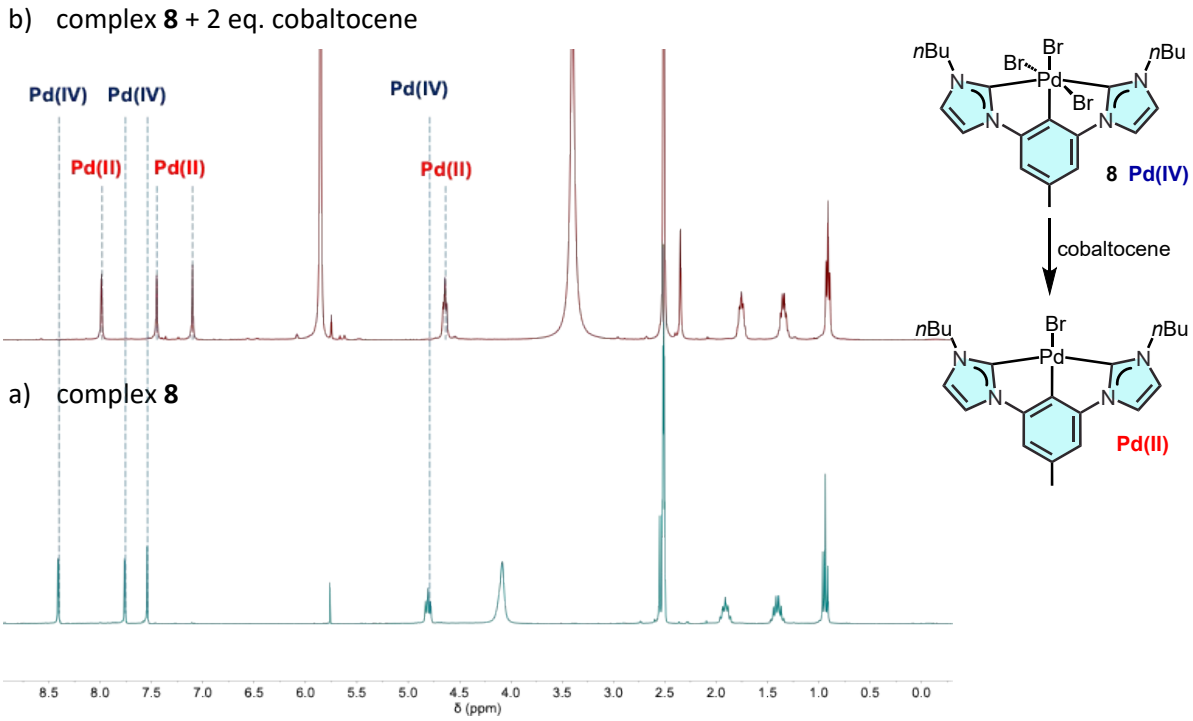

Figure S43. Selected region of the ^{1}H NMR spectra of complex **8** in DMSO-d_6 (a) and upon the addition of 2 equivalents of cobaltocene (b)

8. Bromine transfer from Pd(IV) complexes to styrene

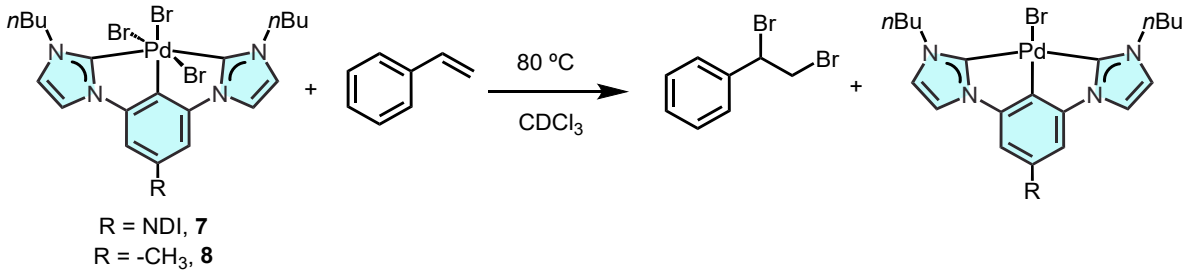

R = NDI, **7**
R = -CH_3, **8**

Scheme S2. Bromine transfer reactions from Pd(IV) complex **7**/**8** to styrene

General Procedure: Complex **7** (7.0 mg, $6.98x10^{-3}$ mmol) or **8** (4.7 mg, $6.98x10^{-3}$ mmol) and styrene (4.0 μL, 0.0349 mmol) were placed together in a Wilmad quick pressure valve NMR tube with 0.8 mL of $CDCl_3$, either in the absence or in the presence of 5 equivalents of TBAF·$3H_2O$. The reaction mixture was heated at 80 ºC for 10 hours, recording a ^{1}H NMR spectrum every 5 minutes. The evolution of the reaction was monitored using a Wilmad coaxial NMR tube charged with 1,3,5-trimethoxybenzene.

Figure S44 shows a selected region of the ^{1}H NMR spectra of the **7**/styrene 1:5 mixture at the beginning of the reaction (Figure S44a) and after 10 hours (Figure S44b). The resulting products, namely 1,2-dibromoethyl)benzene and complex **9**, are conveniently assigned in Figure S44b. As can be seen in Figure S45, in the presence of TBAF·$3H_2O$, there is not bromine transfer to styrene while Pd(IV) complex **7** is reduced to its Pd(II) counterpart **9**.

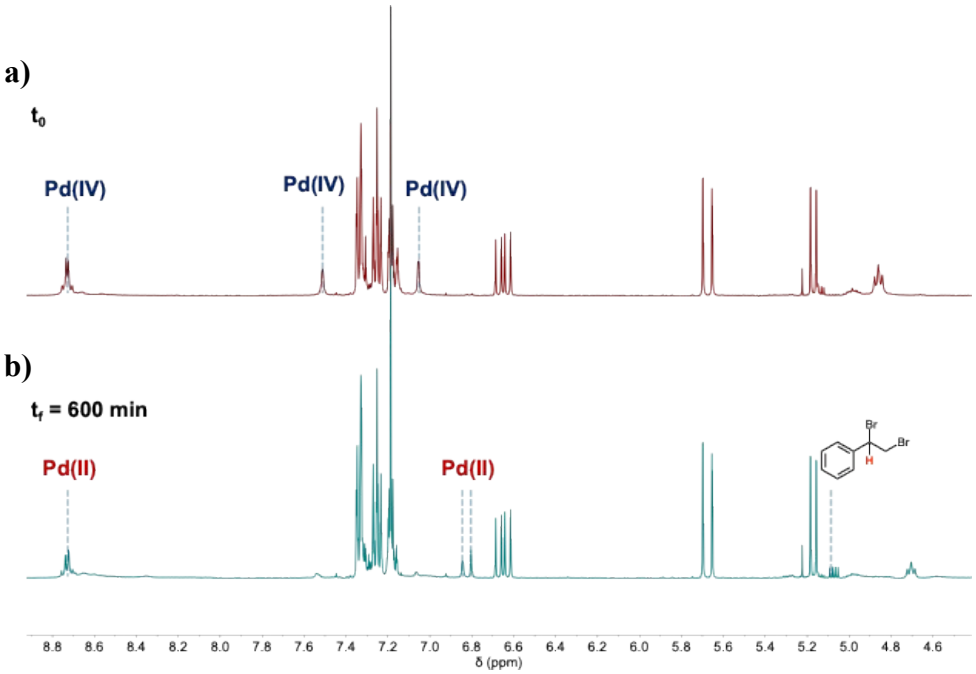

Figure S44. Selected region of the ^{1}H NMR spectra showing the evolution of the rection of complex **7** with styrene in the absence of TBAF·$3H_2O$

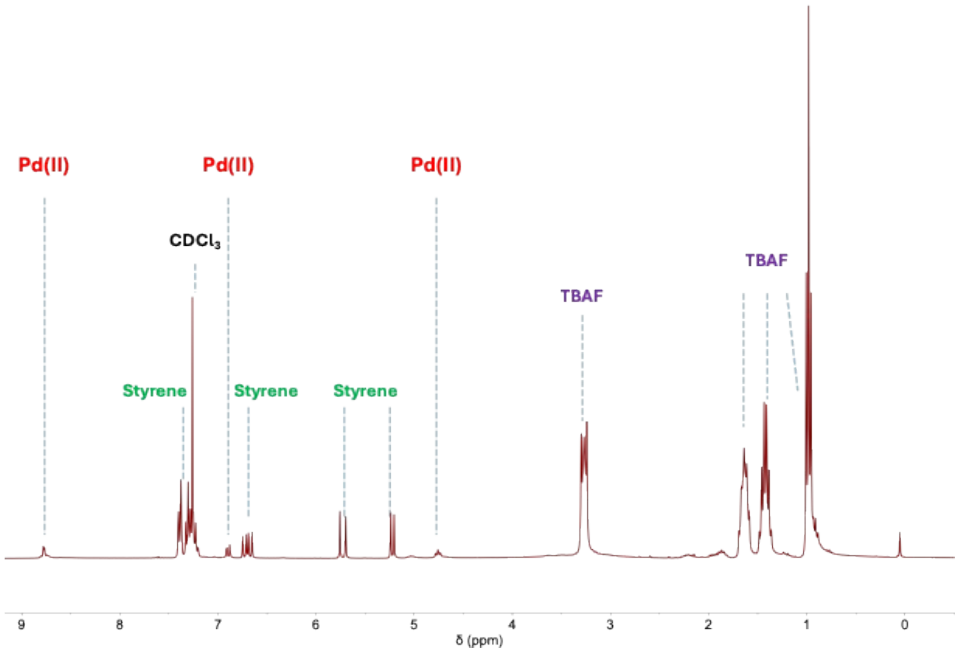

Figure S45. Selected region of the ^{1}H NMR spectra showing the evolution of the rection of complex **7** with styrene in the presence of TBAF·$3H_2O$

9. Catalytic studies

9.1. Pd(II)-mediated homo-cross dehydrogenative coupling of 2-phenylpyridine

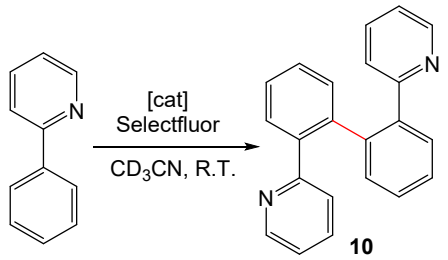

Scheme S3. Homo-cross dehydrogenative coupling (CDC) of 2-phenylpyridine

General procedure. All the catalytic experiments and manipulations were conducted under air atmosphere. In a thick-walled glass tube fitted with a Teflon cap, the catalyst (5.0 mol% of complex **4** or **5**) was added to a 0.111 M solution of 2-phenylpyridine (0.222 mmol) and Selectfluor (0.666 mmol) in CD_3CN (2 mL). The reaction mixture was analyzed by ^1H NMR spectroscopy taking an aliquot (25 μL) at the desired times. Products were identified according to previously reported spectroscopic data.[7] The experiments were carried out in the presence and in the absence of TBAF·$3H_2O$ (5 equiv. and 10 equiv. with respect to the Pd(II) complex).

Blank experiments. Blank experiments were carried out as described above employing complex **4** as catalyst in the absence of Selectfluor or employing Selectfluor in the absence of complex **4**. In both cases, no reaction was observed.

Redox switching experiments. This experiment was carried out following the general procedure described above. After monitoring the reaction for 100 min, TBAF·$3H_2O$ was added to the mixture (10 equiv. with respect to **4**). After collecting data for 50 min, a chemical oxidant, namely $NOBF_4$ was added to the mixture (10 equiv. with respect to **4**).

9.2. Determination of the reaction order with respect to complex 4

The reaction order with respect to complex **4** was determined by plotting the concentration of the product against a normalized time scale t[cat]^n (being n the order of the catalyst), according to the method developed by Dr. Burés.[8] Visual analysis of the reaction profiles depicted in Figure S46 indicated a first order in **4** (Figure S46c).

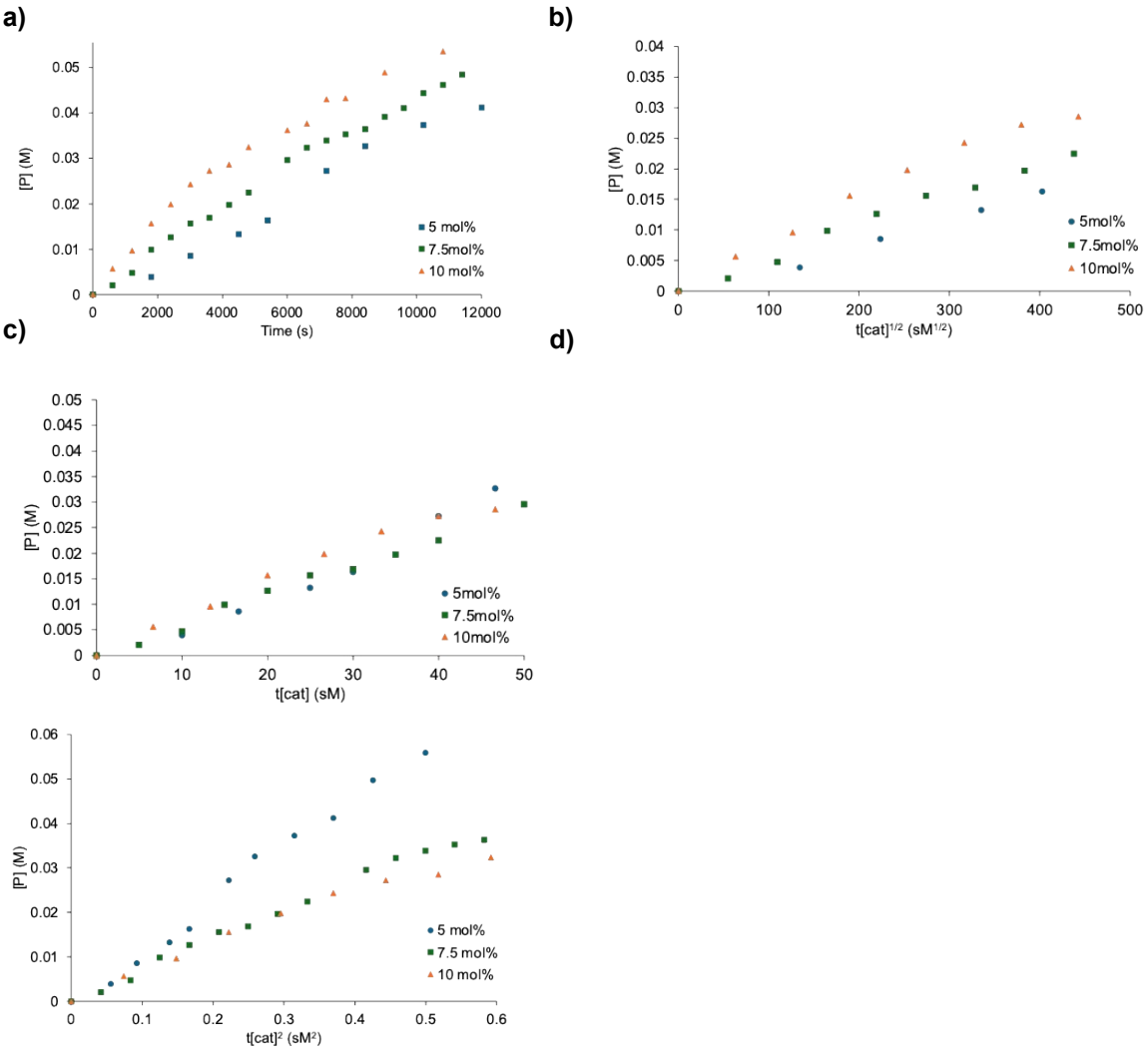

Figure S46. (a) Time-dependent reaction profile of the homo-CDC of 2-phenylpyridine using **4**. (b) Reaction profile with normalized time scale assuming a half-order order in **4**. (c) Reaction profile with normalized time scale assuming a first-order order in **4**. (d) Reaction profile with normalized time scale assuming a second order in **4**.

9.3. Determination of the reaction order with respect to 2-phenylpyridine

The reaction order with respect to 2-phenylpyridine was determined by plotting the concentration of the product against a normalized time scale $t[P]^n$ (being n the order in the 2-phenylpyridine), according to the method developed by Dr. Burés.[8] Visual analysis of the reaction profiles depicted in Figure S47 indicated a zeroth order to 2-phenylpyridine (Figure S47a).

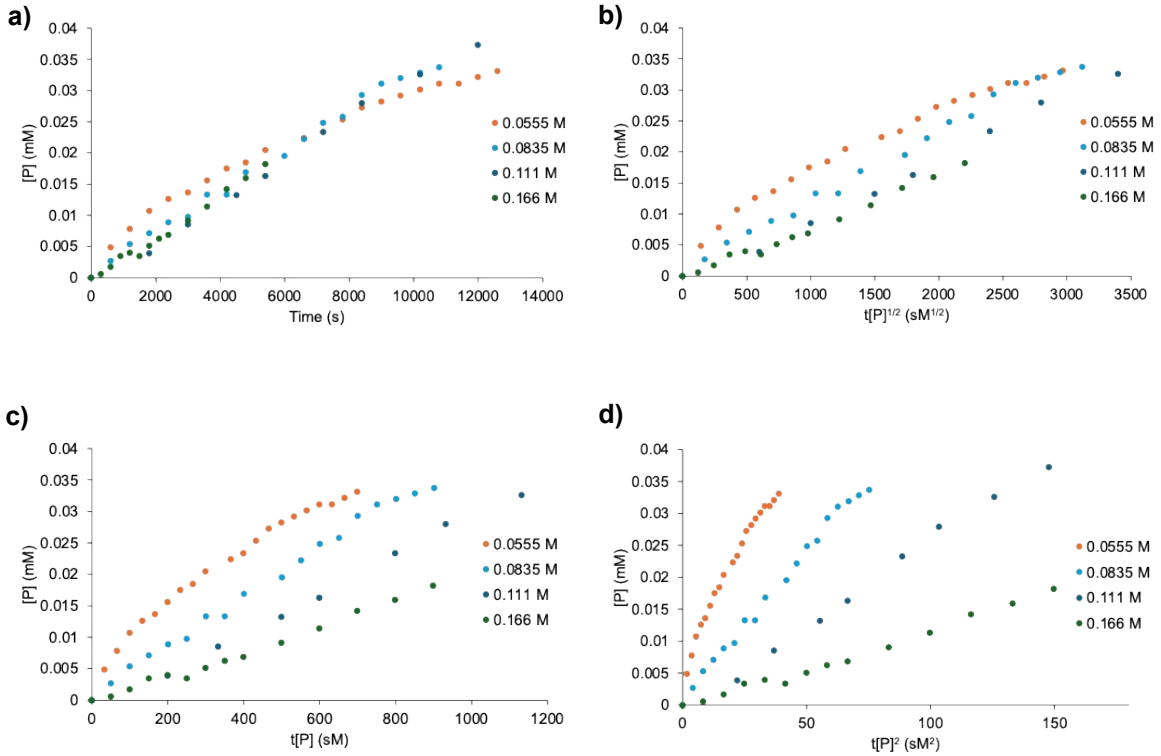

Figure S47. (a) Time-dependent reaction profile of the homo-CDC of 2-phenylpyridine using **4**. (b) Reaction profile with normalized time scale assuming a half-order order in 2-phenylpyridine. (c) Reaction profile with normalized time scale assuming a first-order order in 2-phenylpyridine. (d) Reaction profile with normalized time scale assuming a second order in 2-phenylpyridine.

9.4. Study of the scope of the reaction

The reactions were carried out following the general procedure described in section 8.1. In a thick-walled glass tube fitted with a Teflon cap, the catalyst (5.0 mol% of complex **4**) was added to a 0.111 M solution of the corresponding 2-aryl-N-heterocycle and Selectfluor (0.666 mmol) in CD_3CN (2 mL). The reaction mixture was analyzed by ^1H NMR spectroscopy taking an aliquot (25 μL) after 12 hours of reaction. Products were identified according to previously reported spectroscopic data.[7]

Table S5. Pd(II)-mediated homo-CDC of 2-aryl-N-heterocycles

Entry	2-Aryl-N-heterocycles	Yield(%)
1	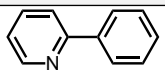	78
2	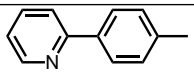	52
3	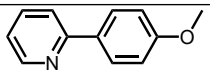	82
4	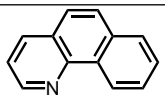	89

10. References

1 S. Martínez-Vivas, D. G. Gusev, M. Poyatos and E. Peris, *Angew. Chem., Int. Ed.*, 2023, e202313899.
2 T. Fujiyama, K. Sugimoto and S. Michuri, *Novel compound and organic electronic device using such compound*, 2006, E. P. Office, WO 2005/09291.
3 O. V. Dolomanov, L. J. Bourhis, R. J. Gildea, J. A. K. Howard and H. Puschmann, *J. Appl. Crystallogr.*, 2009, **42**, 339-341.
4 L. Palatinus and G. Chapuis, *J. Appl. Crystallogr.*, 2007, **40**, 786-790.
5 G. M. Sheldrick, *Acta Crystallogr. A*, 2015, **71**, 3-8.
6 M. Krejcik, M. Danek and F. Hartl, *J. Electroanal. Chem.*, 1991, **317**, 179-187.
7 L. H. Gao, S. Feuillastre, G. Clavier and G. Pieters, *Eur. J. Org. Chem.*, 2023, **26**.
8 a) J. Bures, *Angew. Chem. Int. Ed.*, 2016, **55**, 2028-2031; b) J. Bures, *Angew. Chem., Int. Ed.*, 2016, **55**, 16084-16087.